ISSN 1949-8470 (online)

World Journal of *Radiology*

World J Radiol 2011 May 28; 3(5): 125-146

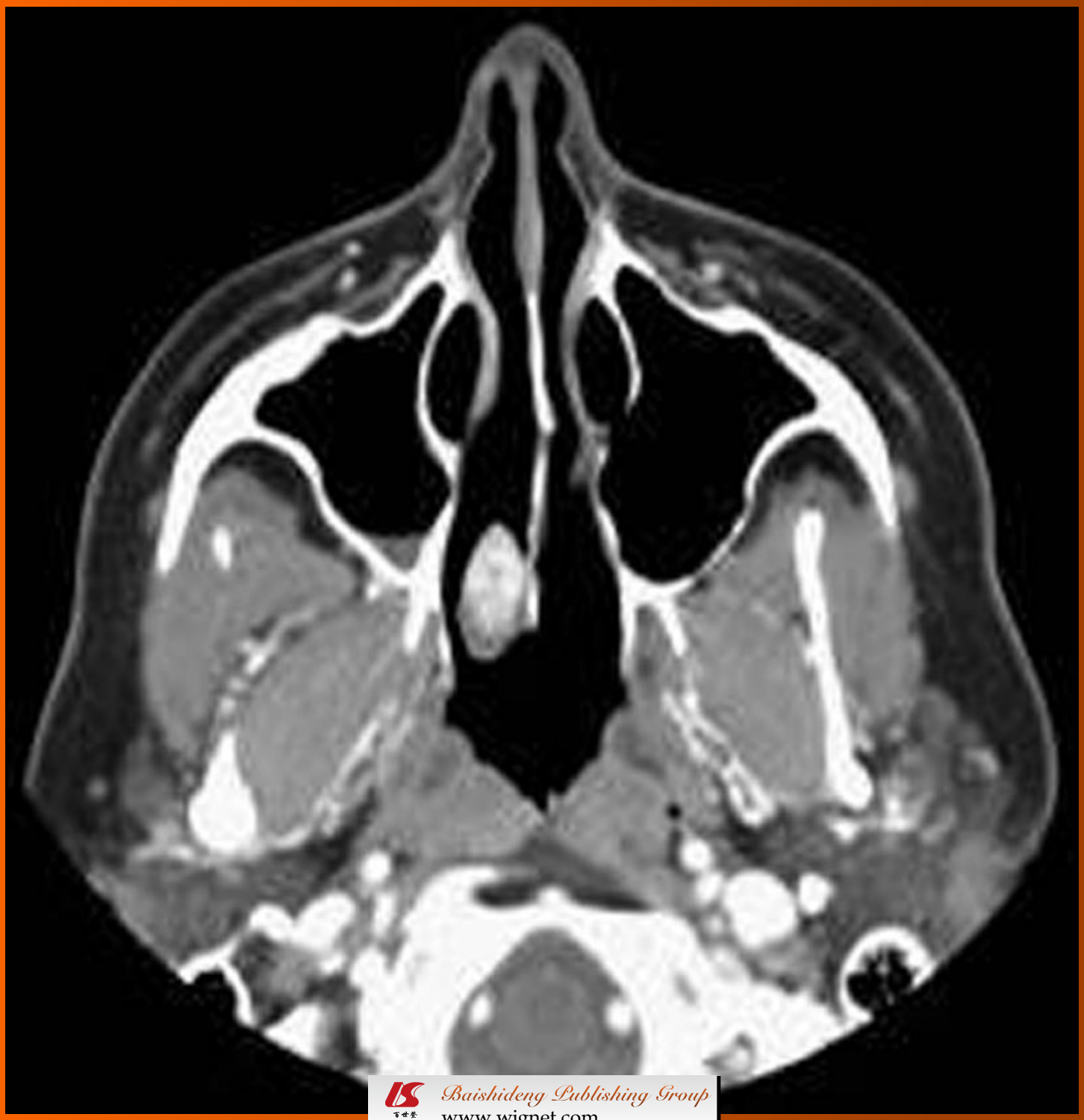

Baishideng Publishing Group
www.wjgnet.com

WJR World Journal of Radiology

A peer-reviewed, online, open-access journal of Radiology

Editorial Board

2009-2013

The *World Journal of Radiology* Editorial Board consists of 319 members, representing a team of worldwide experts in radiology. They are from 40 countries, including Australia (3), Austria (4), Belgium (5), Brazil (3), Canada (9), Chile (1), China (25), Czech (1), Denmark (1), Egypt (4), Estonia (1), Finland (1), France (6), Germany (17), Greece (8), Hungary (1), India (9), Iran (5), Ireland (1), Israel (4), Italy (28), Japan (14), Lebanon (1), Libya (1), Malaysia (2), Mexico (1), Netherlands (4), New Zealand (1), Norway (1), Saudi Arabia (3), Serbia (1), Singapore (2), Slovakia (1), South Korea (16), Spain (8), Switzerland (5), Thailand (1), Turkey (20), United Kingdom (16), and United States (82).

France

Alain Chapel, *Fontenay-Aux-Roses*
Nathalie Lassau, *Villejuif*
Youlia M Kirova, *Paris*
Géraldine Le Duc, *Grenoble Cedex*
Laurent Pierot, *Reims*
Frank Pilleul, *Lyon*
Pascal Pommier, *Lyon*

Germany

Ambros J Beer, *München*
Thomas Deserno, *Aachen*
Frederik L Giesel, *Heidelberg*
Ulf Jensen, *Kiel*
Markus Sebastian Juchems, *Ulm*
Kai U Juergens, *Bremen*
Melanie Kettering, *Jena*
Jennifer Linn, *Munich*
Christian Lohrmann, *Freiburg*
David Maintz, *Münster*
Henrik J Michaely, *Mannheim*
Oliver Micke, *Bielefeld*
Thoralf Niendorf, *Berlin-Buch*
Silvia Obenauer, *Duesseldorf*
Steffen Rickes, *Halberstadt*
Lars V Baron von Engelhardt, *Bochum*
Goetz H Welsch, *Erlangen*

Greece

Panagiotis Antoniou, *Alexandroupolis*
George C Kagadis, *Rion*
Dimitris Karacostas, *Thessaloniki*
George Panayiotakis, *Patras*
Alexander D Rapidis, *Athens*
C Triantopoulou, *Athens*
Ioannis Tsalafoutas, *Athens*
Virginia Tsapaki, *Anixi*
Ioannis Valais, *Athens*

Hungary

Peter Laszlo Lakatos, *Budapest*

India

Anil Kumar Anand, *New Delhi*
Surendra Babu, *Tamilnadu*
Sandip Basu, *Bombay*
Kundan Singh Chufal, *New Delhi*
Shivanand Gamanagatti, *New Delhi*
Vimoj J Nair, *Haryana*
R Prabhakar, *New Delhi*
Sanjeeb Kumar Sahoo, *Orissa*

Iran

Vahid Reza Dabbagh Kakhki, *Mashhad*
Mehran Karimi, *Shiraz*
Farideh Nejat, *Tehran*
Alireza Shirazi, *Tehran*
Hadi Rokni Yazdi, *Tehran*

Ireland

Joseph Simon Butler, *Dublin*

Israel

Amit Gefen, *Tel Aviv*
Eyal Sheiner, *Be'er-Sheva*
Jacob Sosna, *Jerusalem*
Simcha Yagel, *Jerusalem*

Italy

Mohssen Ansarin, *Milan*
Stefano Arcangeli, *Rome*
Tommaso Bartalena, *Imola*
Filippo Cademartiri, *Parma*
Sergio Casciaro, *Lecce*
Laura Crocetti, *Pisa*
Alberto Cuocolo, *Napoli*
Mirko D'Onofrio, *Verona*
Massimo Filippi, *Milan*
Claudio Fiorino, *Milano*
Alessandro Franchello, *Turin*
Roberto Grassi, *Naples*
Stefano Guerriero, *Cagliari*
Francesco Lassandro, *Napoli*
Nicola Limbucci, *L'Aquila*
Raffaele Lodi, *Bologna*
Francesca Maccioni, *Rome*
Laura Martincich, *Candiolo*
Mario Mascalchi, *Florence*
Roberto Miraglia, *Palermo*
Eugenio Picano, *Pisa*
Antonio Pinto, *Naples*
Stefania Romano, *Naples*
Luca Saba, *Cagliari*
Sergio Sartori, *Ferrara*
Mariano Scaglione, *Castel Volturno*
Lidia Strigari, *Rome*
Vincenzo Valentini, *Rome*

Japan

Shigeru Ehara, *Morioka*
Nobuyuki Hamada, *Chiba*
Takao Hiraki, *Okayama*
Akio Hiwatashi, *Fukuoka*
Masahiro Jinzaki, *Tokyo*
Hiroshi Matsuda, *Saitama*
Yasunori Minami, *Osaka*
Jun-Ichi Nishizawa, *Tokyo*
Tetsu Niwa, *Yokohama*
Kazushi Numata, *Kanagawa*
Kazuhiko Ogawa, *Okinawa*
Hitoshi Shibuya, *Tokyo*
Akira Uchino, *Saitama*
Haiquan Yang, *Kanagawa*

Lebanon

Aghiad Al-Kutoubi, *Beirut*

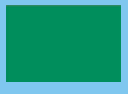

Libya

Anuj Mishra, *Tripoli*

Malaysia

R Logeswaran, *Cyberjaya*
Kwan-Hoong Ng, *Kuala Lumpur*

Mexico

Heriberto Medina-Franco, *Mexico City*

Netherlands

Jurgen J Fütterer, *Nijmegen*
Raffaella Rossin, *Eindhoven*
Paul E Sijens, *Groningen*
Willem Jan van Rooij, *Tilburg*

New Zealand

W Howell Round, *Hamilton*

Norway

Arne Sigmund Borthne, *Lørenskog*

Saudi Arabia

Mohammed Al-Omran, *Riyadh*
Ragab Hani Donkol, *Abha*
Volker Rudat, *Al Khobar*

Serbia

Djordjije Saranovic, *Belgrade*

Singapore

Uei Pua, *Singapore*
Lim CC Tchoyoson, *Singapore*

Slovakia

František Dubecký, *Bratislava*

South Korea

Bo-Young Choe, *Seoul*
Joon Koo Han, *Seoul*
Seung Jae Huh, *Seoul*
Chan Kyo Kim, *Seoul*
Myeong-Jin Kim, *Seoul*
Seung Hyup Kim, *Seoul*
Kyoung Ho Lee, *Gyeonggi-do*
Won-Jin Moon, *Seoul*
Wazir Muhammad, *Daegu*
Jai Soung Park, *Bucheon*
Noh Hyuck Park, *Kyunggi*
Sang-Hyun Park, *Daejeon*
Joon Beom Seo, *Seoul*
Ji-Hoon Shin, *Seoul*
Jin-Suck Suh, *Seoul*
Hong-Gyun Wu, *Seoul*

Spain

Eduardo J Aguilar, *Valencia*
Miguel Alcaraz, *Murcia*
Juan Luis Alcazar, *Pamplona*
Gorka Bastarrika, *Pamplona*
Rafael Martínez-Monge, *Pamplona*
Alberto Muñoz, *Madrid*
Joan C Vilanova, *Girona*

Switzerland

Nicolau Beckmann, *Basel*
Silke Grabherr, *Lausanne*
Karl-Olof Lövblad, *Geneva*
Tilo Niemann, *Basel*
Martin A Walter, *Basel*

Thailand

Sudsriluk Sampatchalit, *Bangkok*

Turkey

Olus Api, *Istanbul*
Kubilay Aydin, *İstanbul*
Işıl Bilgen, *Izmir*
Zulkif Bozgeyik, *Elazig*
Barbaros E Çil, *Ankara*
Gulgun Engin, *Istanbul*
M Fatih Evcimik, *Malatya*
Ahmet Kaan Gündüz, *Ankara*
Tayfun Hakan, *Istanbul*
Adnan Kabaalioglu, *Antalya*
Fehmi Kaçmaz, *Ankara*
Musturay Karcaaltincaba, *Ankara*
Osman Kizilkilic, *Istanbul*
Zafer Koc, *Adana*
Cem Onal, *Adana*
Yahya Paksoy, *Konya*
Bunyamin Sahin, *Samsun*
Ercument Unlu, *Edirne*
Ahmet Tuncay Turgut, *Ankara*
Ender Uysal, *Istanbul*

United Kingdom

K Faulkner, *Wallsend*
Peter Gaines, *Sheffield*
Balaji Ganeshan, *Brighton*
Nagy Habib, *London*
Alan Jackson, *Manchester*
Pradesh Kumar, *Portsmouth*
Tarik F Massoud, *Cambridge*
Igor Meglinski, *Bedfordshire*
Robert Morgan, *London*
Ian Negus, *Bristol*
Georgios A Plataniotis, *Aberdeen*
N J Raine-Fenning, *Nottingham*
Manuchehr Soleimani, *Bath*
MY Tseng, *Nottingham*
Edwin JR van Beek, *Edinburgh*
Feng Wu, *Oxford*

United States

Athanassios Argiris, *Pittsburgh*
Stephen R Baker, *Newark*
Lia Bartella, *New York*
Charles Bellows, *New Orleans*
Walter L Biffl, *Denver*
Homer S Black, *Houston*
Wessam Bou-Assaly, *Ann Arbor*
Owen Carmichael, *Davis*
Shelton D Caruthers, *St Louis*
Yuhchyau Chen, *Rochester*
Melvin E Clouse, *Boston*
Ezra Eddy Wyssam Cohen, *Chicago*
Aaron Cohen-Gadol, *Indianapolis*
Patrick M Colletti, *Los Angeles*
Kassa Darge, *Philadelphia*
Abhijit P Datir, *Miami*
Delia C DeBuc, *Miami*
Russell L Deter, *Houston*
Adam P Dicker, *Phil*
Khaled M Elsayes, *Ann Arbor*
Steven Feigenberg, *Baltimore*
Christopher G Filippi, *Burlington*
Victor Frenkel, *Bethesda*
Thomas J George Jr, *Gainesville*
Patrick K Ha, *Baltimore*
Robert I Haddad, *Boston*
Walter A Hall, *Syracuse*
Mary S Hammes, *Chicago*
John Hart Jr, *Dallas*
Randall T Higashida, *San Francisco*
Juebin Huang, *Jackson*
Andrei Iagaru, *Stanford*
Craig Johnson, *Milwaukee*
Ella F Jones, *San Francisco*
Csaba Juhasz, *Detroit*
Riyad Karmy-Jones, *Vancouver*
Daniel J Kelley, *Madison*
Amir Khan, *Longview*
Euishin Edmund Kim, *Houston*
Vikas Kundra, *Houston*
Kennith F Layton, *Dallas*
Rui Liao, *Princeton*
CM Charlie Ma, *Philadelphia*
Nina A Mayr, *Columbus*
Thomas J Meade, *Evanston*
Steven R Messé, *Philadelphia*
Nathan Olivier Mewton, *Baltimore*
Feroze B Mohamed, *Philadelphia*
Koenraad J Mortele, *Boston*
Mohan Natarajan, *San Antonio*
John L Nosher, *New Brunswick*
Chong-Xian Pan, *Sacramento*
Dipanjan Pan, *St Louis*
Martin R Prince, *New York*
Reza Rahbar, *Boston*
Carlos S Restrepo, *San Antonio*
Veronica Rooks, *Honolulu*
Maythem Saeed, *San Francisco*
Edgar A Samaniego, *Palo Alto*
Kohkan Shamsi, *Doylestown*
Jason P Sheehan, *Charlottesville*
William P Sheehan, *Willmar*
Charles Jeffrey Smith, *Columbia*
Monvadi B Srichai-Parsia, *New York*
Dan Stoianovici, *Baltimore*
Janio Szklaruk, *Houston*
Dian Wang, *Milwaukee*
Jian Z Wang, *Columbus*
Liang Wang, *New York*
Shougang Wang, *Santa Clara*
Wenbao Wang, *New York*
Aaron H Wolfson, *Miami*
Gayle E Woloschak, *Chicago*
Ying Xiao, *Philadelphia*
Juan Xu, *Pittsburgh*
Benjamin M Yeh, *San Francisco*
Terry T Yoshizumi, *Durham*
Jinxing Yu, *Richmond*
Jianhui Zhong, *Rochester*

WJR World Journal of Radiology

Contents

Monthly Volume 3 Number 5 May 28, 2011

World Journal of Radiology
Volume 3 Number 5 May 28, 2011

Contents

NAME OF JOURNAL
World Journal of Radiology

LAUNCH DATE
December 31, 2009

SPONSOR
Beijing Baishideng BioMed Scientific Co., Ltd.,
Room 903, Building D, Ocean International Center,
No. 62 Dongsihuan Zhonglu, Chaoyang District,
Beijing 100025, China
Telephone: +86-10-8538-1892
Fax: +86-10-8538-1893
E-mail: baishideng@wjgnet.com
http://www.wjgnet.com

EDITING
Editorial Board of *World Journal of Radiology*,
Room 903, Building D, Ocean International Center,
No. 62 Dongsihuan Zhonglu, Chaoyang District,
Beijing 100025, China
Telephone: +86-10-8538-1892
Fax: +86-10-8538-1893
E-mail: wjr@wjgnet.com
http://www.wjgnet.com

PUBLISHING
Baishideng Publishing Group Co., Limited,
Room 1701, 17/F, Henan Building,
No.90 Jaffe Road, Wanchai, Hong Kong, China
Fax: +852-3115-8812
Telephone: +852-5804-2046
E-mail: baishideng@wjgnet.com
http://www.wjgnet.com

SUBSCRIPTION
Beijing Baishideng BioMed Scientific Co., Ltd.,
Room 903, Building D, Ocean International Center,
No. 62 Dongsihuan Zhonglu, Chaoyang District,
Beijing 100025, China
Telephone: +86-10-8538-1892
Fax: +86-10-8538-1893
E-mail: baishideng@wjgnet.com
http://www.wjgnet.com

PUBLICATION DATE
May 28, 2011

ISSN
ISSN 1949-8470 (online)

EDITORIAL OFFICE
Na Ma, Director
World Journal of Radiology
Room 903, Building D, Ocean International Center,
No. 62 Dongsihuan Zhonglu, Chaoyang District,
Beijing 100025, China
Telephone: +86-10-8538-1892
Fax: +86-10-8538-1893
E-mail: wjr@wjgnet.com
http://www.wjgnet.com

INSTRUCTIONS TO AUTHORS
Full instructions are available online at http://www.wjgnet.com/1949-8470/g_info_20100316162358.htm.

ONLINE SUBMISSION
http://www.wjgnet.com/1949-8470office

World Journal of Radiology

Online Submissions: http://www.wjgnet.com/1949-8470office
wjr@wjgnet.com
doi:10.4329/wjr.v3.i5.125

World J Radiol 2011 May 28; 3(5): 125-134
ISSN 1949-8470 (online)

EDITORIAL

Imaging appearance of bone tumors of the maxillofacial region

Ahmed Abdel Khalek Abdel Razek

Ahmed Abdel Khalek Abdel Razek, Department of Diagnostic Radiology, Mansoura Faculty of Medicine, Mansoura 3512, Egypt
Author contributions: Abdel Razek AAK contributed solely to the paper.
Correspondence to: Ahmed Abdel Khalek Abdel Razek, MD, Department of Diagnostic Radiology, Mansoura Faculty of Medicine, 62 ElNokrasi Street Meet Hadr, Mansoura 3512, Egypt. arazek@mans.edu.eg
Telephone: +20-50-2326688 Fax: +20-50-2315105
Received: November 18, 2010 Revised: April 25, 2011
Accepted: May 2, 2011
Published online: May 28, 2011

Abstract

This paper reviews the imaging appearance of benign and malignant bone tumors of the maxillofacial region. A benign bone tumor commonly appears as a well circumscribed lesion. The matrix of the tumor may be calcified or sclerotic. Malignancies often display aggressive characteristics such as cortical breakthrough, bone destruction, a permeative pattern and associated soft-tissue masses. Computed tomography scan is an excellent imaging modality for accurate localization of the lesion, characterization of the tumor matrix and detection of associated osseous changes such as bone remodeling, destruction or periosteal reaction. Magnetic resonance imaging is of limited value in the evaluation of maxillofacial bone tumors.

Key words: Benign; Bone; Imaging; Malignant; Tumor

Peer reviewer: Shu-Hang Ng, MD, Professor, Department of Diagnostic Radiology, Chang Gung Medical Center at Linkou, 5 Fuhsing St. Kueisan Hsiang, Taoyuan Hsien 333, Taiwan, China

Abdel Razek AAK. Imaging appearance of bone tumors of the maxillofacial region. *World J Radiol* 2011; 3(5): 125-134 Available from: URL: http://www.wjgnet.com/1949-8470/full/v3/i5/125.htm DOI: http://dx.doi.org/10.4329/wjr.v3.i5.125

INTRODUCTION

A spectrum of benign and malignant bone tumors may be seen in the maxillofacial region. Knowledge of the pathologic features of these tumors and how these features are reflected in their imaging appearance is essential for diagnosis. Familiarity with the imaging appearance, common location, age and gender of bone tumors of the maxillofacial region facilitates the diagnosis and helps radiologists to narrow the list of differential diagnoses and allows for definitive diagnosis in some cases. Early diagnosis of bone tumors is crucial in promoting aggressive treatment, often allowing complications to be avoided[1-4].

Computed tomography (CT) is commonly used for imaging the maxillofacial region. A bone window algorithm better delineates the details of a bony lesion. CT scanning is sensitive for detecting calcified tumor matrix, bone changes and cortical destruction. Magnetic resonance (MR) imaging is not frequently used for the diagnosis of bony maxillofacial lesions. Routine T2- and T1-weighted images and a post-contrast study may be used for the diagnosis of soft tissue lesions with bony tumors[2-5].

Bone tumors of the maxillofacial region may arise from osteogenic, chondrogenic, fibrogenic, vascular, hematopoietic and other elements of the bone. Table 1 shows the World Health Organization classification of benign and malignant bone tumors of the maxillofacial region[6]. Table 2 shows the imaging appearance of bone tumors of the maxillofacial region.

The aim of this article is to review the imaging features of bone tumors of the maxillofacial region.

BENIGN TUMOR

Osteoma

Osteoma is the most common osseous tumor in the maxillofacial region. Osteoma is most commonly seen in the 5th to 6th decades of life and the male-to-female ratio is 1.3:1. Osteoma occurs more commonly in the fronto-ethmoidal sinus and is rarely seen in the maxillary and sphenoid sinuses[2]. All osteomas contain three main components: compact bone (ivory), cancellous bone (trabeculae), and fibrous (spongy) tissue. Osteomas are named according to the dominant component. Compact osteomas most often involve the frontal sinus and grow gradually. Cancellous osteomas are located mostly in the maxillary and ethmoid sinuses and grow relatively quickly. Osteomas are slow growing benign tumors. Multiple craniofacial osteomas may be a part of Gardner syndrome. It is usually asymptomatic but may be associated with facial swelling, deformity, mucocele, proptosis, ocular disturbances and pneumocephalus[2,7]. Osteoma appears as a characteristic sharp, well delineated sclerotic lesion attached by a broad base or pedicle to the bone. Osteoma composed exclusively of compact bone is radiodense (Figure 1), while those containing cancellous bone show evidence of internal trabecular structure. CT multiplanar reconstructions allow the precise identification of the site of origin of the lesion, to fully depict course and patency of all sinus paths, and to correctly assess the integrity of thin bony walls such as the lamina papyracea or the cribriform plate. Compact osteomas produce a complete signal void on all MR sequences, so they are often indistinguishable from the surrounding air in the paranasal sinuses and are thus overlooked. Fibrous osteomas have low to absent signal intensity on all MR sequences[2,4,7,8].

Osteoid osteoma

Osteoid osteoma is a rare tumor in maxillofacial regions (with a few case reports in the ethmoid region) that affects young males in the 2nd to 3rd decades of life. It is a benign osteoblastic lesion characterized by varying intermixtures of osteoid, newly formed bone, and highly vascular supporting osseous tissue (nidus) surrounded by a distinctive surrounding zone of reactive bone formation. Osteoid osteoma appears on CT scan as a characteristic radio-opaque lesion with a nidus (less than 1.5 cm in diameter) which has a radiolucent center surrounded by dense sclerosis. Occasionally, the nidus may have a radio-opaque calcified center with a surrounding radiolucent area. The osteoid osteoma may even be completely sclerotic. MR appearance of osteoid osteoma depends upon the amount of calcification within the nidus, the size of the fibrovascular zone and reactive sclerosis; so it may not be diagnostic. The mass demonstrates patchy enhancement[9].

Osteoblastoma

Osteoblastoma is typically seen in male patients during the 2nd decade of life. It may be seen in the maxilla, ethmoid, nasal cavity and orbit. It shows a marked amount of osteoid tissue produced by osteoblasts. The osteoclasts are numerous and the background is highly vascular. Histologically, osteoblastoma show some similarity to osteoid osteoma, but they are larger without nidus or zonal architecture and show a stronger, more progressive, occasionally even destructive growth; thus, they are sometimes called aggressive osteoblastoma. The patient presents with pain, facial swelling and asymmetry of the face[4,10]. It is commonly seen as an expansile lytic lesion with cortical shell (Figure 2A), or it may show as mixed lytic and sclerotic or predominately sclerotic bone forming a lesion. Ossification foci with ground glass appearance, cloudy confluent mineralization in the central part of the lesion (75%) may be seen. It exhibits intermediate to low signal intensity on T1-weighted images and high to low signal intensity on T2-weighted images depending upon the amount of ossification. Areas of mineralization appear as zones of low signal intensity on T2-weighted images. It shows variable patterns of contrast enhancement[4,10,11] (Figure 2B and C).

Table 1 World Health Organization classification of benign and malignant bone tumors of the maxillofacial region[1]

	Benign	Malignant
Osteogenic	Osteoma	Osteosarcoma
	Osteoid osteoma	
	Osteoblastoma	
Chondrogenic	Chondroblastoma	Chondrosarcoma
	Chondromyxoid fibroma	
	Chondroma	
	Osteochondroma	
Fibrogenic	Fibrous dysplasia	Fibrosarcoma
Vascular	Hemangioma	Hemangioendothelioma
Hematopoietic	-	Plasmacytoma
		Lymphoma
Others	Giant cell tumor	Chordoma
	Aneurysmal bone cyst	Ewing sarcoma
	Meningioma	

Figure 1 Compact Osteoma. Axial computed tomography scan of the paranasal sinus shows a pathognomonic dense sclerotic mass (arrow) in the frontal sinus.

Table 2 Computed tomography and magnetic resonance imaging appearance of bone tumors of the maxillofacial region

	Incidence	Computed tomography	Magnetic resonance imaging
Osteoma	5th-6th decade	Compact: dense sclerotic Cancellous: mixed densities Sharp, well defined lesion attached by a broad base or pedicle to the bone	Compact: signal void Cancellous: low to absent signal
Osteoid osteoma	2nd-3rd decade	Radio lucent nidus (< 1.5 cm) surrounded by dense sclerosis	Non specific signal intensity with patchy enhancement
Osteoblastoma	2nd decade	Expansile lesion with cortical shell May mixed or sclerotic lesion	Non specific signal intensity
Chondroblastoma	More than 30 yr	Lytic lesion with central calcifications and peripheral thin cortical shell	Signal void regions of calcification
Chondromyxoid fibroma	2nd-3rd decade	Well-demarcated expansile lesion with multiple foci of calcification	Signal void regions of calcification
Chondroma	Less than 50 yr	Small polypoid mass with few discrete areas of calcifications	Non specific appearance
Osteochondroma	2nd-4th decade	Mushroom shaped bony outgrowth with calcified cartilagenous cap	Hypointense bony outgrowth with hyperintense cartilaginous cap
Fibrous dysplasia	1st-2nd decade	Ground glass appearance (56%), sclerotic (23%) Lytic with sclerotic margins (21%)	Variable signal intensity depends upon amount of fibrous and sclerotic regions
Giant cell tumor	3rd-4th decade	Expansile mass that tends to destroy and remodel the adjacent bone	Low signal on all sequences
Aneurysmal bone cyst	2nd decade	Lytic expansile lesion with multi-locular "soap bubble" (honey comb) and may fluid–fluid levels	Fluid fluid level with septal enhancement
Hemangioma	2nd decade	Sunburst or spoke wheel pattern of radiating trabeculae	Stippled appearance with intense enhancement
Meningioma	4th decade	Osteoblastic or mixed sclerotic lesion	Low signal on all sequences with intense enhancement
Osteosarcoma	3rd decade	Commonly sclerotic lesion with calcified matrix and sunburst periosteal reaction or it may be mixed or lytic lesion	Signal void of calcification and new bone formation with heterogeneous contrast enhancement
Chondrosarcoma	4th-5th decade	Bony destructive lesion with multiple punctate and stippled calcifications	T2WI: hyperintense areas (chondroid) and hypointense areas (calcified). Curvilinear enhancement
Ewing sarcoma	1st-2nd decade	Destructive aggressive mass with mottled lucent areas and sclerosis and onion peal periosteal reaction	Non specific signal intensity with inhomogeneous enhancement
Fibrosarcoma	3rd-6th decade	Destructive bony lesion, frequently associated with extra osseous soft tissue mass	Low to intermediate signal intensity with inhomogeneous enhancement
Hemangio-endothelioma	2nd decade	Multifocal lytic lesion or dense sclerotic lesion	Tubular signal void structures with intense enhancement
Chordoma	4th decade	Hypodense mass with irregular intratumoral calcifications (30%-50%) with bone destruction	Mixed signal intensity with inhomogeneous enhancement
Lymphoma	4th-7th decade	Lytic, sclerotic or mixed lesions that may be associated with soft tissue mass	Non specific magnetic resonance imaging appearance
Plasmacytoma	4th-7th decade	Well defined bony expansile lesion with intense enhancement	Low SI on T1-weighted images, high on T2-weighted images with intense enhancement
Metastasis	All ages	Radiolucent lesion with cortical destruction. May sclerotic or mixed lytic and sclerotic	Non specific magnetic resonance imaging appearance

SI: Signal intensity

Chondroblastoma

Chondroblastoma is an extremely rare tumor of the maxillofacial region with few case reports. Eighty-three percent of patients with skull chondroblastoma are more than 30 years of age, whereas 92% of patients with chondroblastomas in long bones are less than 30 years of age[12]. It is more commonly seen in the sphenoid and ethmoid and rarely in the maxilla. The tumor is a locally aggressive, well-demarcated expansile lesion. The matrix of the tumor revealed chondroblast and areas of calcification. CT scan confirms the lytic nature of the lesion and shows areas of calcifications in the center and the periphery of the tumor. Areas of low signal intensity on T2-weighted images are secondary to chondroid matrix mineralization. Chondroblastoma of the peripheral skeleton appears to show a different age predilection and characteristically is surrounded by striking peritumoral edema[12,13].

Chondromyxoid fibroma

Chondromyxoid fibroma of the maxillofacial region is typically seen in patients in the 2nd-3rd decade of life with slight female predominance. It is more commonly seen in the maxilla and is unusual in the sphenoid and ethmoid sinuses. The tumor is composed of hypocellular chondroid or myxochondroid tissue with multinucleated giant cells. The CT findings of chondromyxoid fibroma are non specific and almost always suggest a benign lesion. They typically have a lobulated outline with sharp margins, and

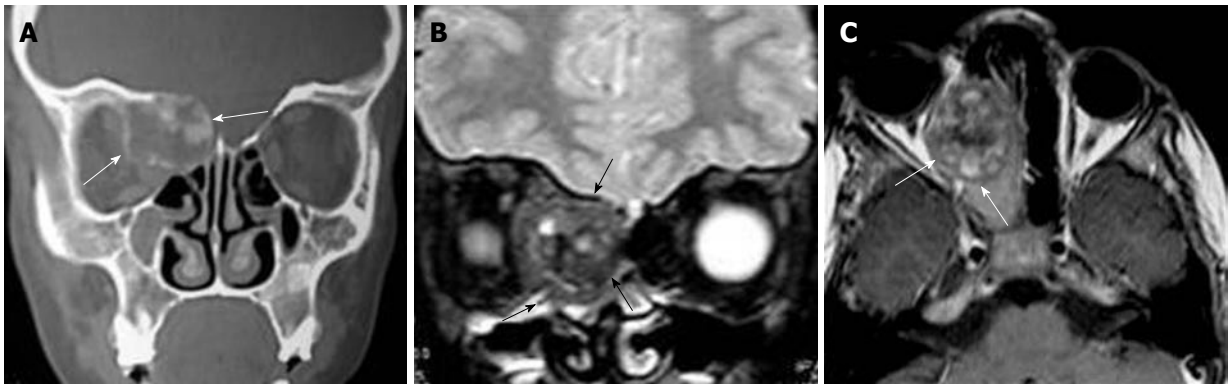

Figure 2 Osteoblastoma. A: Coronal computed tomography shows a nonspecific expansile lesion (arrows) seen in the the right frontoethmoid air cells with extension into the right orbit. It shows ossific foci; B: Coronal T2-weighted image shows a well-defined mass (arrows) in the right ethmoid air cells with extension into the right orbit. It shows nonspecific intermediate to low signal intensity with signal void regions of calcifications and areas of high signal intensity; C: Axial contrast T1-weighted image shows inhomogeneous patterns of enhancement of the lesion (arrows).

Figure 3 Chondromyxoid fibroma. Coronal computed tomography shows expanded mass in the sphenoid sinus with pathognomonic discrete areas of calcification (arrows).

the majority has a sclerotic rim. The cortex of the bone is usually thinned and expanded. In approximately 50% of cases, a portion of the cortex may be absent. Up to one-third of cases show radiographic evidence of soft tissue extension. The majority of tumors have purely lucent matrix. However, approximately 13% of tumors show some discrete areas of calcification (Figure 3). It exhibits low signal intensity on T2-weighted images due to chondroid and myxoid tissue with an inhomogeneous pattern of enhancement[14,15].

Chondroma

Chondroma occurs in patients less than 50 years old of either gender. The most frequent sites of occurrence are the nasal cavity (septum) and ethmoid air cells. It is a polypoid firm, smooth surface nodule measuring from 0-5 to 2 cm and rarely greater than 3 cm. Histologically, it is a lobulated tumor composed of chondrocytes, resembling the normal histology of the hyaline cartilage. The differentiation of chondroma from a well-differentiated chondrosarcoma may at times be difficult if not impossible. It may be differentiated from chondrosarcoma by pathology. It shows discrete areas of calcification on CT scan[5,16].

Osteochondroma

Osteochondroma is an extremely rare tumor of the maxillofacial region. The age of incidence ranges between 10 and 40 years, with most patients presenting in the 3rd decade. The male to female ratio ranges from 1:1 to 2:1. It is located in the facial bones, nasal septum, sphenoid sinus, ethmoid cells and zygomatic arch. The reason for the rare occurrence of osteochodroma in the maxillofacial skeleton is the intramembranous development of these bones. It is a benign cartilage-capped osseous growth composed of compact and cancellous bone. Osteochondromas are characterized by the presence of a cartilage cap on top of the tumor; with time, cartilage tissues gradually undergo endochondral ossification and are replaced by bone. It may be multiple in patients with hereditary multiple exostoses[4]. Osteochondroma usually has a pathognomonic pedunculated mushroom shaped bony outgrowth with peripheral cortex and central cancellous bone that arises from the surface of the bone. The cartilaginous cap may or may not be focally calcified. On MR imaging, it shows a peripheral rim of low signal intensity of the cortical bone and central high signal intensity within the cancellous region. A thin hyperintense cartilagenous cap on T2-weighted images may be seen[4,17].

Fibrous dysplasia

Fibrous dysplasia (FD) represents 2.5% of all osseous and 7% of all benign osseous neoplasms. The craniofacial bones are the affected sites in 10%-25% of patients with monostotic FD and in 50% of patients with polyostotic FD[18]. In addition, the craniofacial region may be affected by a form of FD that is not restricted to a single bone, but may be confined to a single anatomical site. This type of the disease has been termed craniofacial FD. In addition, FD may be a component of McCune-Albright syndrome or it may exhibit cherubism phenotype. The monostotic and polyostotic types are known to be related to mutations in the guanine nucleotide-binding

Figure 4 Fibrous dysplasia. Coronal computed tomography scan shows a well-defined expansile bony lesion involving the left maxilla with characteristic ground glass appearance.

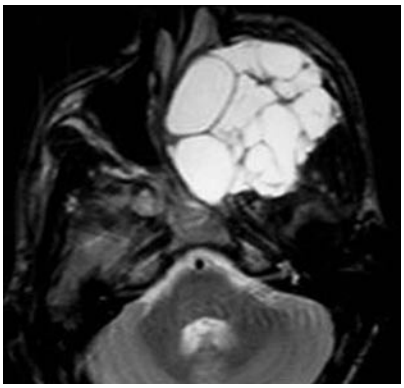

Figure 5 Aneurysmal bone cyst. Axial T2-weighted image shows an expansile multiloculated cystic lesion in the maxillary sinus with multiple septae.

protein gene located on chromosome 20q and the craniofacial subtype has not been localized to this chromosome. It is more commonly seen at the 1st to 2nd decade of life at the floor of the anterior cranial fossa[5,19]. It is located in the frontal bone (82%), sphenoid (71%), ethmoid (68%), and maxillary (28%) bones. Histologically, FD consists of varying amounts of spindle cell bundles and trabeculae of immature woven bone. There is replacement of normal spongiosa and filling of the medullary cavity of affected bones by an abnormal fibrous tissue that contains trabeculae of poorly calcified primitive bone formed by osseous metaplasia. It may be associated with aneurysmal bone cyst. Spontaneous malignant transformation of FD is estimated to occur in less than 1% of cases, and osteosarcoma is the most common histological type, followed by fibrosarcoma, chondrosarcoma and malignant fibrohistiocytoma. These malignancies are most commonly found in the maxilla. Most reported cases of malignant degeneration in FD have occurred after radiation therapy.

The imaging appearance of FD depends upon the amount of fibrous and bony element. CT remains the "gold-standard" imaging modality for FD, allowing characterization of the three main imaging patterns of expanded bone. The cortical bone tends to remain intact, with the FD changes most often found in the medullary bone. The CT findings include: pathognomonic ground glass appearance with bone expansion and alternative radiolucent and radiodensity areas (56%), sclerotic pattern with homogenous radiodensity (23%) and lytic appearance with solitary round or oval, well-defined radiolucent with sclerotic margins (21%) (Figure 4). Sclerotic lesions are homogeneously dense, whereas cyst degeneration is the least common finding and is characterized by a spherical or ovoid lucency surrounded by a dense bony shell. On T1-weighted images, the signal intensity is usually low to intermediate depending on the ratio of fibrous tissue to mineralized matrix. On T2-weighted images, lesions with a highly mineralized matrix show low signal intensities, whereas lesions with high fibrous tissue content and cystic spaces return high signal intensities. The lesion may enhance after contrast administration[5,18-21].

Cherubism is a rare autosomal-dominant disorder resulting from different mutations to FD and is therefore a distinct entity at the molecular level. It occurs in children (2-5 years) and is more common in males. It commonly appears as a bilateral and symmetrical multilocular cystic swelling of the mandible with expansion of the maxilla and involvement of the maxillary sinuses. The signal characteristics on MR imaging of cherubism are nonspecific[22]. Cherubism has been reported in association with neurofibromatosis type 1 and Noonan-like/multiple giant-cell lesion syndrome[23].

Giant cell tumor

Giant cell tumors occur more commonly during the 3rd and 4th decades of life and are more commonly located in the sphenoid but rarely in the ethmoid bones and the maxilla. It is a benign, locally aggressive tumor characterized by osteoclast-like giant cells. Multicentric tumors with an aggressive course or malignant giant cell tumor with metastasis have been reported. There is a high recurrence rate (40%-60%) after resection[24]. Classically, the tumor destroys the bone and appears as a nonspecific rarified area, being a lytic lesion. Although fairly well circumscribed, some cystic changes, ballooning and perforation of the bony cortex may be noted. The area of destruction has a "soap bubble" appearance, with normal trabeculae and little reactive bone at the margin. On MR imaging, it shows fairly low signal intensity on all pulse sequences, and shows moderate to marked contrast enhancement[24,25].

Aneurysmal bone cyst

Aneurysmal bone cyst occurs more commonly in the 2nd decade of life and may be seen in the maxilla, ethmoid, sphenoid bone and periorbital region. These cysts are composed of blood-filled, anastomosing cavernous spaces, separated by cyst-like walls. The precise nature and histogenesis of the aneurysmal bone cyst remains unclear. A primary type has to be differentiated from a secondary form; the latter develops on a preexisting

bone lesion such as giant cell tumor, osteoblastoma, or chondroblastoma in 1/3 of patients[3,26]. It appears as an expansile, multi-locular "soap bubble" (honey comb) radio-lucency, causing expansion of the bony cortex. It is surrounded by a marginal thin shell. MR imaging commonly shows cystic spaces with internal septa (Figure 5) and septal contrast enhancement. Fluid-fluid levels of varying intensities might be present and should not be considered diagnostic, as this finding might be present in giant cell tumor, telangiectatic osteosarcoma, and chondroblastoma[26,27].

Intraosseous (central) hemangioma

Intraosseous hemangioma can occur at any age with the peak incidence being in the 2nd decade of life. An estimated 2:1 female to male ratio has been documented. These tumors occur more commonly in the maxilla and nasal bones and may be found in the orbit. It is a hamartoma with anomalous proliferation of endothelial-lined vascular channels. Hemangiomas are classified into capillary, cavernous and mixed sub-types, depending on the predominant type of vascular channel. It is usually asymptomatic. The characteristic "spoke-wheel", "wagon-wheel", "corduroy" or "sunburst" appearance on CT scan arises from thickening of pre-existing trabeculae, secondary to intramembranous bone affected by the vascular channels. T1-weighted images characteristically show hypointensity of the lesion. T2-weighted images reveal heterogeneous hyperintensity within the lesion. A stippled appearance is seen in the tumor matrix. The tumor enhances, intensely or heterogeneously, after the administration of contrast material[28,29].

Intraosseous (central) meningioma

Intra-osseous meningioma forms 1% of all meningiomas that typically occur in the 4th decade of life with female predominance. It is more commonly seen in the orbit and sphenoid ridge and rarely involved in the paranasal sinuses. It is more commonly seen as an osteoblastic or mixed sclerotic lesion. It shows a hyperostotic form that may be associated with inward bulging of the inner table and surface irregularity of the hyperostotic bone. CT is the investigation of choice to detect the tumor, cortical destruction and both intra- and extra-osseous extension. At MR imaging, there is bone thickening that exhibits low signal intensity on all pulse sequences with intense contrast enhancement[30,31].

MALIGNANT TUMOR

Osteosarcoma

Fewer than 10% of osteosarcomas arise in the craniofacial bones with most such tumors developing in the mandible and maxilla. Typically, the tumor affects males in the 3rd decade and one or two decades later in the appendicular skeleton. Osteosarcomas may involve the mandible or maxilla and rarely the ethmoid region. The most common sites of involvement are the body of the mandible and the alveolar ridge or the antral area of the maxilla. The majority of tumors arise within the medullary cavity of the affected bone with rare examples developing on the bony surfaces. It may be secondary to radiation, fibrous dysplasia, Paget disease, trauma, osteomyelitis, ossifying fibroma and giant cell tumor. Osteosarcoma after radiation typically develops after a latency period of 5-10 years after doses in excess of 3000 Gy. These tumors characteristically occur at the edge of the radiation field because the administered radiation is unable to cause cell death but is sufficient to induce malignant transformation. Osteosarcoma can be classified on location into intramedullary, intracortical, periosteal and parosteal (surface) and extraosseous. It can be further categorized according to the prominent type of matrix tissue observed microscopically such as osteoblastic, chondroblastic, fibroblastic, telengectatic and osteoclast-rich types[32,33]. On CT, the tumor displays a spectrum of bone changes from well demarcated borders, notably the low grade osteosarcoma (uncommon), to lytic bone destruction with indefinite margin and variable cortical bone erosion, to the ostoeblastic form, where the bone is sclerotic. The majority of osteosarcomas have matrix mineralization, calcifications of the osteoid or osteoid-like substance within the tumor and some tumors show a sunburst effect caused by radiating mineralized tumor spiculae. Cortical breakthrough and interruption of alveolar margin is common in advanced cases. On MR

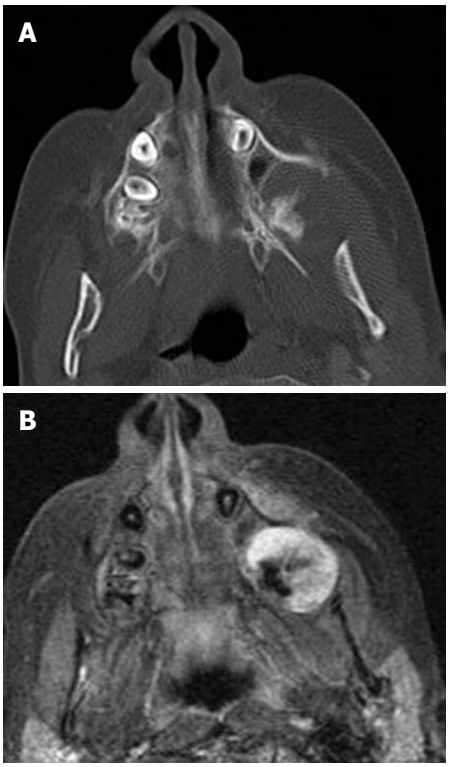

Figure 6 Osteosarcoma. A: Axial computed tomography shows a rather irregular characteristic spiculated mass in the left alveolar margin of the maxilla adjacent to the lateral pterygoid plate; B: Axial contrast T1-weighted image shows inhomogeneous enhancement of the mass with non-enhanced signal void regions of calcification (Courtesy of Castillo M).

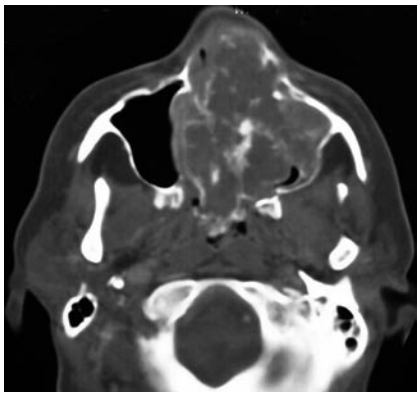

Figure 7 Chondrosarcoma. Axial computed tomography shows bulky mass in the nasal cavity and left maxillary sinus with characteristic stippled and amorphous areas of calcification (arrows).

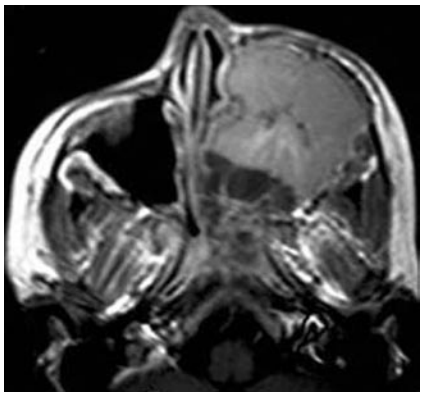

Figure 8 Ewing Sarcoma. Axial contrast T1-weighted image shows a large destructive mass occupying the entire left maxillary sinus. The mass shows inhomogeneous non-specific pattern of contrast enhancement.

imaging, osteosarcoma is of low to intermediate signal intensity on T1-weighted images and is of high signal intensity on T2-weighted images. Calcifications and new bone formations appear as signal void regions within the lesion that show inhomogeneous patterns of contrast enhancement[1,32-34] (Figure 6).

Chondrosarcoma

Craniofacial chondrosarcoma accounts for 2% of all chondrosarcomas with a peak incidence during the 4th to 5th decades of life and a male to female ratio of 2.4:1. It is seen in the skull base (common), maxilla and orbit (less common), and cartilage of the nasal septum (rarely). Chrondosarcoma has been reported to develop in association with malignant conditions, such as osteosarcoma, fibrosarcoma, and leukemia, as well as benign conditions, such as Paget disease and fibrous dysplasia[35]. Histologically, chondrosarcoma of the craniofacial region can be divided into subtypes: the conventional subtype with myxoid and/or hyaline components, the aggressive mesenchymal and dedifferentiated subtype and the extremely rare clear cell subtype. The conventional type, which is the most common form, is slow growing, and rarely metastatic. On the other hand, mesenchymal chondrosarcoma is more aggressive and tends to metastasize. They slowly increase in size, and the majority of them are already extensive at the time of diagnosis[36]. On CT scan, chondrosarcoma shows a soft tissue mass with characteristic multiple stippled and amorphous areas of calcifications that may be associated with bone destruction and an inhomogeneous pattern of contrast enhancement (Figure 7). The signal intensity of the chondroid matrix is lower than bone matrix on T1-weighted images. There are hyperintense areas (chondroid tissue) and hypointense areas (calcified regions) on T2-weighted images. The tumor may show characteristic curvilinear septal enhancement of fibrovascular tissue and non-ossified cartilage[1,35-37]. The development of metastases varies among studies and ratios of metastases are between 14% and 90%, with the lungs being the preferred site. Regional cervical lymph node metastases are reported in not more than 5% of all cases.

Ewing sarcoma

Craniofacial Ewing sarcoma accounts for 1%-4% of all Ewing sarcomas with peak incidence between 5 and 20 years old in either sex, although it does have a predication for whites[38]. It may be seen in the orbital wall, sphenoid and maxilla. It is an aggressive, malignant, small round cell tumor of bone. Because of the intense vascularity of the tumor, hemorrhage and necrosis are common. Marked tumor necrosis is considered a poor prognostic factor. The commonest sites of metastases are the lungs and the skeleton that occur in the early course of the disease. Ewing sarcomas appear as a destructive aggressive mass with mottled irregular lucent areas interposed with some sclerosis. The margin is diffuse with unsharp edges and extensive cortical destruction. It may be associated with perpendicular bony spicules and shows the characteristic onion peel appearance of periosteal reaction, and less often with a sunburst type of periosteal reaction. The tumor tends to metastasize early, often to multiple other bony sites and the lungs. On MR imaging, the tumor is heterogeneously hypointense on T1-weighted and heterogeneously hyperintense on T2-weighted scans. On post-contrast T1-weighted images, the lesion shows heterogeneous signal increase with internal hypointense necrotic areas[1,39,40] (Figure 8).

Fibrosarcoma

Craniofacial fibrosarcoma is very rare and is seen in the 3rd to 6th decades of life with a slight male predominance. The infantile variant that is seen in patients less than 5 years has a better prognosis. It is rarely seen in the maxilla. It may be central (medullary) or peripheral (periosteal). It is a malignant tumor with variable fibrous intracellular substances devoid of bone or cartilage formation. On CT, fibrosarcoma is a destructive lesion of variable size, frequently associated with extra osseous soft tissue mass. On MR imaging, the tumor shows low or intermediate signal intensity on both T1- and T2-weighted

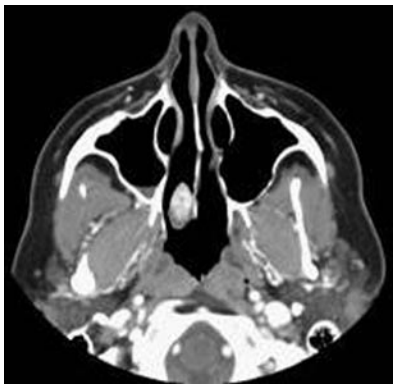

Figure 9 Hemangioendothelioma. Axial computed tomography shows a non-specific sclerotic enhanced lesion related to the posterior part of the nasal septum on the right side (Courtesy of Castillo M).

images with an inhomogeneous pattern of contrast enhancement[1,41].

Hemangioendothelioma

Hemangioendothelioma of the maxillofacial region is a low-grade, malignant vascular tumor. Hemangioendotheliomas account for only 0.5% to 1.0% of malignant primary bone tumors. Most of them arise in the third decade and they are prone to occur in the maxillary sinus. Multifocality is present in 9%-14% of cases. The tumor is often large and aggressive. Multifocal lytic lesions (honeycomb appearance), aggressive bony destruction with expansion, dense sclerotic lesion and soft-tissue mass are seen on CT scan (Figure 9). There is a low to intermediate signal intensity on T1-weighted images and slightly high signal intensity on T2-weighted images. Tubular signal-void regions represent blood vessels that may be seen within the lesion. It shows moderate to marked contrast enhancement[42].

Chordoma

Chordoma forms 1% of all intracranial tumors that are typically seen in male patients during the 4th decade of life. It is commonly located in the clivus and may extend into the sphenoid and maxillary sinus. It is a benign, locally invasive tumor. It appears as a hypodense mass with irregular intratumoral calcifications (30%-50%) that are associated with variable contrast enhancement and bone destruction. The tumor shows intermediate signal intensity with areas of high signal representing hemorrhage or high protein cystic areas on T1-weighted images. The lesion has relatively high signal intensity associated with areas of low signal intensity that may be seen in the lesion that represents residual fragments or sequestrations of bone on T2-weighted images. After contrast administration, it shows inhomogeneous patterns of enhancement[4,43,44].

Lymphoma

Lymphoma of the maxillofacial region occurs over a broad age range (4th-7th decades) with slight male predominance. The vast majority are large B cell non-Hodgkin lymphomas. On CT scan, lymphoma can produce lytic, sclerotic or mixed lesions that may be associated with soft tissue mass. It appears as isointense to muscles on both T1- and T2-weighted images that are associated with soft tissue mass. The mass shows intense patterns of contrast enhancement. Burkitt's lymphoma is a special type that may be seen in Africans during the 1st decade of life. It appears as an osteolytic lesion with periosteal reaction and perpendicular spicules of new bone in the maxilla. An extra-osseous soft tissue mass may develop parallel with bone destruction[1,2,45].

Solitary intramedullary plasmacytoma

Plasma cell disorders are characterized by the accumulation of monoclonal plasma cells that produce the same immunoglobulin. Plasmacytomas are plasma cell tumors. They can occur as solitary tumors outside the bone marrow (solitary medullary (bone) plasmacytomas, solitary extramedullary plasmacytomas, but can also be associated with multiple myeloma. Solitary medullary plasmacytoma occurs more commonly in male patients between the 4th and 7th decades of life. It may be seen in the sphenoid sinus and the maxilla. It is a fairly well defined expansile lesion with contrast enhancement. It exhibits low signal intensity on T1-weighted images and high or mixed signal intensity on T2-weighted images with marked contrast enhancement that may simulate meningioma[2,46].

Metastasis

Metastasis is uncommon in the maxillofacial region. The maxillary sinus is most frequently involved (33%) followed by the sphenoid (22%), ethmoid (14%) and frontal (9%) sinuses. In 22% of cases, multiple sinuses are involved. The most common tumor sites to disseminate to this region are the kidney (40%), lung (9%), breast (8%), thyroid (8%) and prostate (7%). The remaining 28% of cases include multiple miscellaneous sites. In 10-15% of cases, the metastases are limited to the nasal cavity. Although the eventual outcome is usually poor, prognosis depends, in part, on whether the sinonasal metastasis is isolated or part of widespread disseminated disease. Metastasis may appear as a localized, well-defined radiolucent lesion in a slow growing lesion, or it may be associated with cortical destruction in a highly aggressive lesion, osteoblastic in breast cancer or mixed lytic or sclerosis in patients with prostate cancer. The tumor exhibits low signal intensity on T1-weighted images and high signal intensity on T2-weighted images that may be associated with an enhancing soft tissue mass[1,47,48].

CONCLUSION

We conclude that imaging plays an important role in the diagnosis of bone tumors of the maxillofacial region. CT scan is an excellent imaging modality for accurate localization of the lesion, characterization of the tumor matrix and detection of associated osseous changes such as

bone remodeling, destruction or periosteal reaction. CT scan is sufficient for the diagnosis of most bone tumors of the maxillofacial region. However, MR imaging is of limited value as bone tumors display a non-specific imaging appearance.

ACKNOWLEDGMENTS

We thank Mauricio Castillo, MD, Professor of Radiology at University of North Carolina, Chapel Hill, NC, United States of America for his help with some of the figures in this article.

REFERENCES

1 **Weber AL**, Bui C, Kaneda T. Malignant tumors of the mandible and maxilla. *Neuroimaging Clin N Am* 2003; **13**: 509-524
2 **Theodorou DJ**, Theodorou SJ, Sartoris DJ. Primary nonodontogenic tumors of the jawbones: an overview of essential radiographic findings. *Clin Imaging* 2003; **27**: 59-70
3 **Boeddinghaus R**, Whyte A. Current concepts in maxillofacial imaging. *Eur J Radiol* 2008; **66**: 396-418
4 **Borges A**. Skull base tumours Part II. Central skull base tumours and intrinsic tumours of the bony skull base. *Eur J Radiol* 2008; **66**: 348-362
5 **Wenig BM**, Mafee MF, Ghosh L. Fibro-osseous, osseous, and cartilaginous lesions of the orbit and paraorbital region. Correlative clinicopathologic and radiographic features, including the diagnostic role of CT and MR imaging. *Radiol Clin North Am* 1998; **36**: 1241-1259, xii
6 **Dorfman HD**, Czerniak B, Kotz R, Vanel D, Park YK, Unni KK. WHO classification of tumours of bone: Introduction. In: Fletcher CDM, Unni KK, Mertens F, editors. World health organization classification of tumours: Pathology and genetics of tumours of soft tissue and bone. Lyon: IARC Press, 2002: 227-232
7 **Earwaker J**. Paranasal sinus osteomas: a review of 46 cases. *Skeletal Radiol* 1993; **22**: 417-423
8 **Dalambiras S**, Boutsioukis C, Tilaveridis I. Peripheral osteoma of the maxilla: report of an unusual case. *Oral Surg Oral Med Oral Pathol Oral Radiol Endod* 2005; **100**: e19-e24
9 **Lachanas VA**, Koutsopoulos AV, Hajiioannou JK, Bizaki AJ, Helidonis ES, Bizakis JG. Osteoid osteoma of the ethmoid bone associated with dacryocystitis. *Head Face Med* 2006; **2**: 23
10 **Lee EJ**, Park CS, Song SY, Park NH, Kim MS. Osteoblastoma arising from the ethmoidal sinus. *AJR Am J Roentgenol* 2004; **182**: 1343-1344
11 **Park YK**, Kim EJ, Kim SW. Osteoblastoma of the ethmoid sinus. *Skeletal Radiol* 2007; **36**: 463-467
12 **Madhup R**, Srivastava M, Srivastava AN, Bhatt MLB, Kirti S. Chondroblastoma of maxilla. *Oral Oncol Extra* 2005; **41**: 159-161
13 **Al Mestady RM**, Alorainy IA, El Watidy SM, Arafah MM. Intracranial extraosseous chondroblastoma simulating meningioma. *AJNR Am J Neuroradiol* 2007; **28**: 1880-1881
14 **Hashimoto M**, Izumi J, Sakuma I, Iwama T, Watarai J. Chondromyxoid fibroma of the ethmoid sinus. *Neuroradiology* 1998; **40**: 577-579
15 **Kadom N**, Rushing EJ, Yaun A, Santi M. Chondromyxoid fibroma of the frontal bone in a teenager. *Pediatr Radiol* 2009; **39**: 53-56
16 **Kurozumi N**, Kamiishi H. Nasal chondroma: a case report. *Br J Plast Surg* 1984; **37**: 247-249
17 **Wu W**, Hu X, Lei D. Giant osteochondroma derived from pterygoid process of sphenoid. *Int J Oral Maxillofac Surg* 2007; **36**: 959-962
18 **Celenk P**, Zengin Z, Muglali M, Celenk C. Computed tomography of cranio-facial fibrous dysplasia. *Eur J Radiol Extra* 2009; **69**: e85-e87
19 **Mohammadi-Araghi H**, Haery C. Fibro-osseous lesions of craniofacial bones. The role of imaging. *Radiol Clin North Am* 1993; **31**: 121-134
20 **MacDonald-Jankowski DS**. Fibro-osseous lesions of the face and jaws. *Clin Radiol* 2004; **59**: 11-25
21 **Chong VF**, Khoo JB, Fan YF. Fibrous dysplasia involving the base of the skull. *AJR Am J Roentgenol* 2002; **178**: 717-720
22 **Beaman FD**, Bancroft LW, Peterson JJ, Kransdorf MJ, Murphey MD, Menke DM. Imaging characteristics of cherubism. *AJR Am J Roentgenol* 2004; **182**: 1051-1054
23 **Martínez-Tello FJ**, Manjón-Luengo P, Martin-Pérez M, Montes-Moreno S. Cherubism associated with neurofibromatosis type 1, and multiple osteolytic lesions of both femurs: a previously undescribed association of findings. *Skeletal Radiol* 2005; **34**: 793-798
24 **Lee HJ**, Lum C. Giant-cell tumor of the skull base. *Neuroradiology* 1999; **41**: 305-307
25 **Tang JY**, Wang CK, Su YC, Yang SF, Huang MY, Huang CJ. MRI appearance of giant cell tumor of the lateral skull base: a case report. *Clin Imaging* 2003; **27**: 27-30
26 **Fyrmpas G**, Constantinidis J, Televantou D, Konstantinidis I, Daniilidis J. Primary aneurysmal bone cyst of the maxillary sinus in a child: case report and review of the literature. *Eur Arch Otorhinolaryngol* 2006; **263**: 695-698
27 **Bathla G**, Chowdhury V, Dixit R, Kottiyath VC, Jain R. Aneurysmal bone cyst of ethmoid sinus: Uncommon manifestation of a rare case. *Eur J Radiol Extra* 2009; **70**: e49-e51
28 **Vargel I**, Cil BE, Kiratli P, Akinci D, Erk Y. Hereditary intraosseous vascular malformation of the craniofacial region: imaging findings. *Br J Radiol* 2004; **77**: 197-203
29 **Koulouris G**, Rao P. Multiple congenital cranial hemangiomas. *Skeletal Radiol* 2005; **34**: 485-489
30 **Daffner RH**, Yakulis R, Maroon JC. Intraosseous meningioma. *Skeletal Radiol* 1998; **27**: 108-111
31 **Tokgoz N**, Oner YA, Kaymaz M, Ucar M, Yilmaz G, Tali TE. Primary intraosseous meningioma: CT and MRI appearance. *AJNR Am J Neuroradiol* 2005; **26**: 2053-2056
32 **Lee YY**, Van Tassel P, Nauert C, Raymond AK, Edeiken J. Craniofacial osteosarcomas: plain film, CT, and MR findings in 46 cases. *AJR Am J Roentgenol* 1988; **150**: 1397-1402
33 **Park YK**, Ryu KN, Park HR, Kim DW. Low-grade osteosarcoma of the maxillary sinus. *Skeletal Radiol* 2003; **32**: 161-164
34 **Vlychou M**, Ostlere SJ, Kerr R, Athanasou NA. Low-grade osteosarcoma of the ethmoid sinus. *Skeletal Radiol* 2007; **36**: 459-462
35 **Chen CC**, Hsu L, Hecht JL, Janecka I. Bimaxillary chondrosarcoma: clinical, radiologic, and histologic correlation. *AJNR Am J Neuroradiol* 2002; **23**: 667-670
36 **Nemec SF**, Donat MA, Hoeftberger R, Matula C, Czerny C. Chondrosarcoma of the petrous apex: A diagnostic and therapeutic challenge. *Eur J Radiol Extra* 2005; **54**: 87-91
37 **Dass AN**, Peh WC, Shek TW, Ho WK. Case 139: nasal septum low-grade chondrosarcoma. *Radiology* 2008; **249**: 714-717
38 **Worch J**, Matthay KK, Neuhaus J, Goldsby R, DuBois SG. Ethnic and racial differences in patients with Ewing sarcoma. *Cancer* 2010; **116**: 983-988
39 **Özer C**, Arpacı T, Yıldız A, Apaydın FD, Duce MN, Düzovalı Ö. Primary Ewing's sarcoma of the paranasal sinus with intracranial and intraorbital extension. *Eur J Radiol Extra* 2005; **55**: 47-50
40 **Howarth KL**, Khodaei I, Karkanevatos A, Clarke RW. A sinonasal primary Ewing's sarcoma. *Int J Pediatr Otorhinolaryngol* 2004; **68**: 221-224
41 **O'Connell TE**, Castillo M, Mukherji SK. Fibrosarcoma arising in the maxillary sinus: CT and MR features. *J Comput Assist*

Tomogr 1996; **20**: 736-738
42 **Rosen A**, Glaser AY, Respler D. Hemangioendothelioma of the orbit in a 3-month-old infant. *Inter J Pediatr Otorhinolaryngol Extra* 2006; **1**: 188-191
43 **Shugar JM**, Som PM, Krespi YP, Arnold LM, Som ML. Primary chordoma of the maxillary sinus. *Laryngoscope* 1980; **90**: 1825-1830
44 **Erdem E**, Angtuaco EC, Van Hemert R, Park JS, Al-Mefty O. Comprehensive review of intracranial chordoma. *Radiographics* 2003; **23**: 995-1009
45 **Weber AL**, Rahemtullah A, Ferry JA. Hodgkin and non-Hodgkin lymphoma of the head and neck: clinical, pathologic, and imaging evaluation. *Neuroimaging Clin N Am* 2003; **13**: 371-392
46 **Wein RO**, Popat SR, Doerr TD, Dutcher PO. Plasma cell tumors of the skull base: four case reports and literature review. *Skull Base* 2002; **12**: 77-86
47 **Green S**, Som PM, Lavagnini PG. Bilateral orbital metastases from prostate carcinoma: case presentation and CT findings. *AJNR Am J Neuroradiol* 1995; **16**: 417-419
48 **Ogawa T**, Hara K, Kawarai Y, Nishizaki K, Nomiya S, Takeda Y, Akagi H, Kariya S. A case of infantile neuroblastoma with intramucosal metastasis in a paranasal sinus. *Int J Pediatr Otorhinolaryngol* 2000; **55**: 61-64

S- Editor Cheng JX **L- Editor** Webster JR **E- Editor** Zheng XM

World Journal of Radiology

Online Submissions: http://www.wjgnet.com/1949-8470office
wjr@wjgnet.com
doi:10.4329/wjr.v3.i5.135

World J Radiol 2011 May 28; 3(5): 135-140
ISSN 1949-8470 (online)

BRIEF ARTICLE

Abdominal crush injury in the Sichuan earthquake evaluated by multidetector computed tomography

Tian-Wu Chen, Zhi-Gang Yang, Zhi-Hui Dong, Heng Shao, Zhi-Gang Chu, Si-Shi Tang

Tian-Wu Chen, Zhi-Gang Yang, Zhi-Hui Dong, Heng Shao, Zhi-Gang Chu, Si-Shi Tang, Department of Radiology, West China Hospital of Sichuan University, Chengdu 610041, Sichuan Province, China

Tian-Wu Chen, Sichuan Province Key Laboratory of Medical Imaging, and Department of Radiology, Affiliated Hospital of North Sichuan Medical College, Nanchong 637000, Sichuan Province, China

Author contributions: Chen TW, Yang ZG, Dong ZH, Shao H, Chu ZG and Tang SS designed the research; Chen TW, Dong ZH, Shao H and Chu ZG performed the research; Yang ZG and Tang SS contributed analytic tools; Chen TW, Dong ZH and Chu ZG analyzed the data; Chen TW and Yang ZG wrote the paper; Chen TW, Yang ZG, Dong ZH, Shao H, Chu ZG and Tang SS revised the paper.

Supported by The National Natural Science Foundation of China, No. 30870688 and the Science Foundation for Distinguished Young Scholars of Sichuan Province, No. 2010JQ0039

Correspondence to: Zhi-Gang Yang, MD, Department of Radiology, West China Hospital of Sichuan University, 37# Guo Xue Xiang, Chengdu 610041, Sichuan Province, China. yangzg1117@yahoo.com.cn
Telephone: +86-28-85423817 Fax: +86-28-85423817

Received: February 20, 2011 Revised: March 24, 2011
Accepted: May 1, 2011
Published online: May 28, 2011

Abstract

AIM: To investigate the features of abdominal crush injuries resulting from an earthquake using multidetector computed tomography (MDCT).

METHODS: Fifty-one survivors with abdominal crush injuries due to the 2008 Sichuan earthquake underwent emergency non-enhanced scans with 16-row MDCT. Data were reviewed focusing on anatomic regions including lumbar vertebrae, abdominal wall soft tissue, retroperitoneum and intraperitoneal space; and types of traumatic lesions.

RESULTS: Fractures of lumbar vertebrae and abdominal wall soft tissue injuries were more common than retro- and intraperitoneal injuries ($P < 0.05$). With regard to the 49 lumbar vertebral fractures in 24 patients, these occurred predominantly in the transverse process ($P < 0.05$), and 66.67% of patients (16/24) had fractures of multiple vertebrae, predominantly two vertebrae in 62.5% of patients (10/16), mainly in L1-3 vertebrae in 81.63% of the vertebrae (40/49). Retroperitoneal injuries occurred more frequently than intraperitoneal injuries ($P < 0.05$), and renal and liver injuries were most often seen in the retroperitoneum and in the intraperitoneal space, respectively (all $P < 0.05$).

CONCLUSION: Transverse process fractures in two vertebrae among L1-3 vertebrae, injury of abdominal wall soft tissue, and renal injury might be features of earthquake-related crush abdominal injury.

Key words: Abdominal injury; Crush injury; Earthquake; Multidetector computed tomography

Peer reviewer: Yasunori Minami, MD, PhD, Assistant Professor, Division of Gastroenterology and Hepatology, Department of Internal Medicine, Kinki University School of Medicine, 377-2 Ohno-higashi, Osaka-sayama, Osaka, 589-8511, Japan

Chen TW, Yang ZG, Dong ZH, Shao H, Chu ZG, Tang SS. Abdominal crush injury in the Sichuan earthquake evaluated by multidetector computed tomography. *World J Radiol* 2011; 3(5): 135-140 Available from: URL: http://www.wjgnet.com/1949-8470/full/v3/i5/135.htm DOI: http://dx.doi.org/10.4329/wjr.v3.i5.135

INTRODUCTION

An earthquake that registered 8.0 on the Richter scale

devastated the mountainous region of Sichuan in China at 2:28 pm Beijing time on May 12, 2008, and the epifocus was located at Wenchuan County in the Sichuan Province of China. The widespread effect of the earthquake destroyed a significant number of schools, factories, apartments, office areas, and villages. The schools, factories and villages were more vulnerable compared with the other styles of buildings. Due to the high-force impacts of building collapse or falling objects in this earthquake, 374 643 people were injured with 69 227 killed and 17 923 missing. In view of the massive morbidity arising from this event, an undamaged key university hospital 92 kilometers away from the epicenter, equipped with 4300 beds, working as the largest-scale urgent care center in the earthquake-affected areas, received the largest number of injured people, and treated a total of 2728 cases over a period of 15 d. Of these patients, 2.05% (56/2728) had sustained abdominal injury associated with crush injury. Missed abdominal injury or delayed treatment frequently results in preventable mortality, but prompt localization of abdominal injuries in trauma patients can improve the efficacy of injury management[1,2].

To localize suspected blunt abdominal injury, ultrasound is used as an initial tool in most European and Asian-Pacific countries[3]. However, ultrasonography is not sensitive in detecting hollow organ and retroperitoneal injury[4]. Computed tomography (CT) scanning of the abdomen can overcome the limitation of ultrasonography, and is currently considered the gold standard for detecting intra- and retroperitoneal lesions in trauma patients[5-8]. To our knowledge, the features of abdominal crush injuries on CT due to massive earthquake damage have not been reported in the literature, although some relevant publications regarding crush injuries in other anatomic regions have been reported[9-12]. Thus, our aim was to retrospectively investigate the features of abdominal crush injuries resulting from this earthquake using emergency multidetector CT (MDCT) for better understanding and treatment planning of abdominal crush trauma survivors in similar future earthquakes.

MATERIALS AND METHODS

Patients

The local institutional ethic review board approved the present study, and patient informed consent was waived. Patients entered our study according to the following inclusion criteria: (1) victims had abdominal crush injuries in combination with or without injuries in other systems such as the thorax and pelvis; (2) clinical suggested abdominal injuries were initially confirmed by CT; and (3) the etiology of abdominal injuries was crush injury in the 2008 Sichuan earthquake on the basis of the history and the findings of rescue. Patients with abdominal injuries were excluded from the present study if the etiology of the injuries was jumping or accidental falling from buildings based on the history of injury.

Between May 12 and May 26, 2008, fifty-one consecutive survivors (22 men and 29 women; mean age, 41.92 years; age range, 7-86 years) with abdominal crush injuries resulting from the 2008 Sichuan earthquake, who were admitted into this university hospital and met the inclusion criteria, were enrolled in the present study. In the cohort, 49 patients with abdominal crush injuries in combination with crush injuries in one or more other anatomic regions including the thorax, pelvis, extremity and neck were confirmed by MDCT scans in 39, 40, 11 and 4 patients, respectively. In addition, 36 patients including 27 patients with retro- or intraperitoneal visceral injuries had acute renal failure confirmed by the measurement of myoglobin in blood and urine shortly after the CT scans. In order to timely detect the injuries for appropriate emergency treatments in a great number of injured patients, two of five MDCT scanners in the university hospital were utilized to image the abdominal injuries as soon as possible. The mean time from injury to imaging was 5.4 d with a range of 6 h to 14 d. In patients who waited a long time from injury to rescue, few dangerously ill patients survived before being conveyed to the university hospital to receive effective treatments, although some had received antibiotics in the field hospital to prevent infection in the disaster areas. Based on the image findings and clinical data, 37 patients with retro- or intraperitoneal visceral injuries, fracture of lumber vertebra, or severe injury of abdominal wall soft tissue underwent surgery, and the remaining victims received conservative treatment. Owing to appropriate treatments, 49 patients were cured, and 2 patients died of fatal crush injury.

CT

Thirty-eight and thirteen victims with abdominal crush injuries underwent CT scanning with a Philips Brilliance 16-row MDCT (Philips Healthcare, Eindhoven, the Netherlands) and a Siemens Somatom Sensation 16-row MDCT (Siemens Medical Systems, Forchheim, Germany), respectively. An emergency abdominal CT scan without intravenous contrast material was obtained as soon as possible from the right diaphragmatic dome to the pelvic basement. Because we suspected all victims to have abdominal injuries in combination with acute renal failure due to the massive earthquake, the patients did not undergo contrast-enhanced abdominal CT scans in the earthquake situation. The following scanning parameters were used for both scanners to image the injuries: 120 kV, 250 mAs, 0.5-s gantry rotation time, pitch of 0.85, collimation of 16 mm × 0.75 mm, 5-mm reconstructed section thickness, 380-mm field of view, and matrix of 512 mm × 512 mm. When fractures of the lumbar vertebrae were found, the reconstructed section thickness was 1 mm.

Image data analysis

Image data were transferred to a picture archiving communication system (Syngo-Imaging, Siemens Medical Solutions, Forchheim, Germany). Data were retrospectively analyzed by an experienced radiological Associate Profes-

sor (the first author, who had 12 years of experience in radiology) and one experienced radiologist (the third author with 11 years of experience in radiology) working in consensus with emphasis on trauma in anatomic regions including the retroperitoneum, intraperitoneal space, lumbar vertebrae, and abdominal wall soft tissue. Because of lumbar vertebral fractures related to pathological changes in abdominal wall soft tissue, the fractures were reviewed in detail by multiplanar reconstruction with a slab of 5-7 mm and three-dimensional reconstruction. In order to better understand overall types of abdominal injuries, traumatic lesions in parenchymal organs together with peritoneal pathological changes (seroperitoneum and pneumoperitoneum) and injuries of abdominal aorta were reviewed.

Statistical analysis

Statistical analysis was performed with the SPSS statistical package (version 13.0 for Windows, SPSS Inc., Chicago, IL, USA). We compared incidences of lumbar vertebrae and abdominal wall soft tissue crush injuries with those of retro- and intraperitoneal visceral crush injuries using the Chi-square test. If significant differences were found, comparisons in incidences between fractures of lumbar vertebrae and abdominal wall soft tissue injuries, or between retro- and intraperitoneal injuries were performed using similar tests. Additionally, comparisons between incidences of renal and perirenal injuries and incidences of other organ injuries in the retroperitoneal space, or between incidences of liver injuries and incidences of other organ injuries in the intraperitoneal region were also performed using these tests. A *P*-value of less than 0.05 was considered significant.

RESULTS

Predominant anatomic distributions of abdominal crush injuries

In this cohort, lumbar vertebrae or abdominal wall soft tissue injuries occurred in 33.33% (17/51) of victims; retro- or intraperitoneal injuries occurred in 11.76% (6/51) of victims; and both lumbar vertebrae or abdominal wall soft tissue injuries and retro- or intraperitoneal injuries occurred in 54.91% (28/51) of victims. Lumbar vertebrae or abdominal wall soft tissue injuries were more common than retro- or intraperitoneal injuries ($P = 0.017$).

Injuries of lumbar vertebrae appeared as fractures. Fractures of lumbar vertebrae, injuries of abdominal wall soft tissue, and both fractures of lumbar vertebrae and injuries of abdominal wall soft tissue occurred in 33.33% (17/51), 41.18% (21/51) and 11.76% (7/51) of patients, respectively. No statistical differences were found between fractures of lumbar vertebrae and injuries of abdominal wall soft tissue ($P = 0.484$).

In this cohort, patients with retro- or intraperitoneal injuries were composed of retroperitoneal injuries in 35.29% (18/51), intraperitoneal injuries in 9.8% (5/51), and both retro- and intraperitoneal injuries in 21.57% (11/51). Retroperitoneal injuries were more common than intraperitoneal injuries ($P = 0.008$).

Table 1 Cases of crush lumbar vertebral fractures according to the involved anatomic sites of vertebrae (n = 24) n (%)

Anatomic sites of vertebrae involved	Cases of lumbar vertebral fractures
Transverse process	15 (62.5)
The body	1 (4.17)
Transverse process + the body	4 (16.67)
Transverse process + spinous process	1 (4.17)
Transverse process + the body + spinous process	1 (4.17)
Transverse process + the body + vertebral plate	1 (4.17)

Figure 1 In a 41-year-old woman with crush fractures of the transverse process of lumbar vertebrae, the fractures were in combination with a right perirenal hematoma (arrow) and swelling of bilateral psoas muscles (arrowheads).

Lumbar vertebrae fractures vs injuries of abdominal wall soft tissue

Lumbar vertebral crush fractures were detected in a total of 49 vertebrae in 47.06% (24/51) of patients. The fractures occurred in the transverse process (Figure 1), the body, spinous process or vertebral plate of lumber vertebrae. These crush fractures are listed in Table 1. Factures of the transverse process were more common than those of any other anatomic sites of a lumber vertebra ($P < 0.001$).

In this cohort, the mean number of lumbar vertebrae involved per patient with lumbar vertebral crush fractures was 2 vertebrae with the peak prevalence between 1 and 2 of the number affected which ranged from 1 to 5. The cohort was composed of 33.33% of patients (8/24) with fractures of single vertebra and 66.67% (16/24) with fractures of multiple vertebrae. Multiple fractures occurred in two vertebrae in 62.5% of patients (10/16) and in more than two vertebrae in 37.5% (6/16) of patients.

According to the lumbar levels involved, the fractures occurred in L1 vertebra in 26.53% (13/49) of vertebrae, in L2 vertebra in 34.69% (17/49), in L3 vertebra in 20.41% (10/49), in L4 vertebra in 12.24% (6/49), and in L5 vertebra in 6.12% (3/49).

Table 2 Cases of crush retroperitoneal injuries according to the viscera involved and types of lesions (n = 14) n (%)

Retroperitoneal injuries	Cases of crush retroperitoneal injuries
Renal and perirenal injuries	
Perirenal hematoma	4 (28.57)
Subcapsular hematoma	1 (7.14)
Fluid collection in perirenal space	2 (14.29)
Air collection in perirenal space	1 (7.14)
Hemorrhage of renal cyst	1 (7.14)
Pancreatic injury	
Traumatic pancreatitis	2 (14.29)
Pancreatic rupture with hematoma	1 (7.14)
Renal injuries + pancreatic injury	
Renal contusion + pancreatic contusion	1 (7.14)
Renal injuries + injury of abdominal aorta	
Rupture of abdominal aortic aneurysm + perirenal hematoma	1 (7.14)

Table 3 Cases of crush intraperitoneal injuries according to the viscera involved and types of lesions (n = 9) n (%)

Intraperitoneal injuries	Cases of crush intraperitoneal injuries
Liver injuries	
Hepatorrhexis	3 (33.33)
Hepatorrhexis with hematoma	3 (33.33)
Hepatorrhexis with subcapsular hematoma	1 (11.11)
Splenic rupture	
With hematoma	1 (11.11)
With subcapsular hematoma	1 (11.11)

With regard to injuries of abdominal wall soft tissue, these occurred in a total of 28 patients. Intramuscular hematoma, muscular swelling or fatty edema were detected in 64.29% of patients (18/28), and 35.71% of patients (10/28) had both subcutaneous air collection and swelling of abdominal wall soft tissue. According to the anatomic regions involved, injuries of abdominal wall soft tissue occurred in the anterior abdominal wall in 10.71% of patients (3/28), in the posterior abdominal wall in 14.29% (4/28), in the flank abdominal wall in 24.43% (6/28), in both the anterior and posterior abdominal wall in 14.29% (4/28), in the flank and anterior abdominal wall in 10.71% (3/28), in the flank and posterior abdominal wall in 10.71% (3/28), and in the flank and anterior and posterior abdominal wall in 17.86% (5/28).

Retro- vs intraperitoneal injuries

In this cohort, 29 patients had retroperitoneal injuries. The injuries were composed of renal or perirenal injuries (Figure 1), traumatic pancreatitis or pancreatic injury (Figure 2), rupture of abdominal aortic aneurysm, fluid collection in perirenal space and air collection in the posterior perirenal space in a total of 14 patients, and the remaining patients had swelling of perirenal fascia. The detailed results are listed in Table 2. Renal or perirenal injuries were more often seen than injuries of the other organs in the retroperitoneal space ($P < 0.001$).

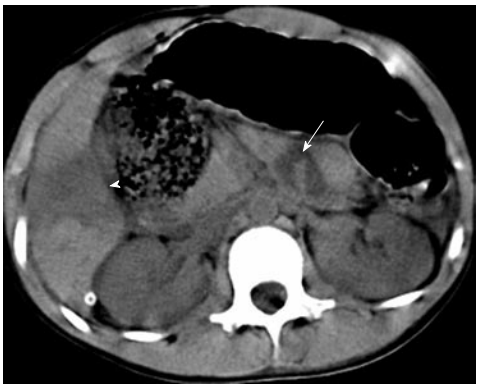

Figure 2 Computed tomography scan obtained at the level of the renal hilum in a 13-year-old girl with crush abdominal injuries demonstrates pancreatic rupture (arrow) and hepatorrhexis (arrowhead) with hematoma.

As for intraperitoneal injuries, 16 patients had intraperitoneal injuries. Intraperitoneal parenchymal injuries were composed of liver injuries (Figure 2) and splenic injuries with or without seroperitoneum and pneumoperitoneum in a total of 9 patients, and the remaining patients were composed of seroperitoneum in 5 patients and pneumoperitoneum in 2 patients. Detailed cases of these results are listed in Table 3. Liver injuries were more often seen than splenic injuries ($P < 0.001$).

Additionally, parenchymal polytraumatism (Figure 2) associated with the earthquake was found in 7.84% (4/51) of patients including injury in bilateral kidneys, in unilateral kidney and liver, in liver and pancreas, and in unilateral kidney and liver and pancreas each in 1 patient.

DISCUSSION

During the past 20 years, natural disasters have claimed more than three million lives worldwide[13]. With respect to loss of life, an earthquake is the most harmful disaster among all types of natural disasters[14]. In the 2008 Sichuan earthquake, 374 643 people were injured. Based on the patients presenting in the university hospital, abdominal crush injuries were one type of injury which occurred in 2.05% (56 of 2728), which was higher than the morbidity (1%) in the 2005 Kashmir earthquake[15]. Based on the largest number of injured people treated in the hospital in the earthquake-affected area, we proposed that the CT features of abdominal crush injuries might be helpful in better understanding and treatment planning of survivors with abdominal crush injuries in similar future earthquakes.

As an emergency imaging tool for diagnosing abdominal crush injuries, MDCT helps to image the injuries as soon as possible in a great number of injured patients due to an increased speed of image acquisition, and significantly reduces the time requirements for initial diagnostic evaluation[16]. We, therefore, focused on the emergency assessment of abdominal injuries using 16-row MDCT scanners in this earthquake setting. Because of the suspicion of acute renal failure associated with crush

syndrome in the massive earthquake, use of iodinated contrast might presumably potentiate the development of renal failure in some patients, and the emergency CT scans of the abdomen were performed without intravenous contrast material.

Clinically, we found that fractures of lumbar vertebrae and injury of abdominal wall soft tissue were more often seen than retro- and intraperitoneal injuries, which may be explained by the fact that some victims with retro- and intraperitoneal injuries may have died before a rescue could be carried out, whereas most victims with fractures of lumbar vertebrae or injury of abdominal wall soft tissue survived long enough to be transported to the hospital to receive effective treatments.

Additionally, we found that retroperitoneal injuries were more common than intraperitoneal injuries. According to Chen *et al*[17], most victims fell down and were trapped in the prone position when the earthquake occurred, and the high-force impacts of collapsed buildings and falling objects frequently struck the lower back, which eventually results in a high frequency of retroperitoneal injuries.

With regard to fractures of lumbar vertebrae, fractures of multiple vertebrae were more often seen than fractures of single vertebra, and occurred most frequently in two vertebrae. Regarding the involved anatomic sites of a vertebra, fractures of the transverse process were more common than those of the body, spinous process and vertebral plate. Based on the vertebral levels involved, L1-3 fractures were more common in patients with crush fractures of lumbar vertebrae, which was consistent with a previous report[9].

As for retroperitoneal parenchymal injuries in the massive earthquake, renal and perirenal injuries were more often seen than injuries to other organs in the retroperitoneal space. According to Sever *et al*[18], the renal victims were of vital importance since they could predict the final outcome as well as be directive for medical therapies. We presumed that the CT findings could help us to better understand renal injuries from the earthquake for effective treatments to improve therapeutic outcome.

As for intraperitoneal parenchymal injuries arising from this earthquake, they were composed of liver and splenic injuries. Liver injuries were more often seen than injuries of any other parenchymal viscera. In addition, seroperitoneum occurred frequently in patients with abdominal crush injury. Full thickness bowel disruption was not represented in the population under study, which may be explained by the fact that victims with lethal injuries died before a rescue was carried out.

In view of the severity of abdominal crush injuries, abdominal parenchymal polytraumatism may be a good indicator. According to Ersoy *et al*[19], multiple injuries were more frequent in nonsurvivors than in survivors during the Marmara earthquake, and polytraumatism was one of the main factors which increased mortality risk in dialyzed injuries after the earthquake. In our study, we found that 7.84% (4/51) of patients had parenchymal polytraumatism. Although the morbidity of victims with abdominal parenchymal polytraumatism was not significant, attention should be paid clinically to prevent high mortality.

There were two inevitable limitations in our study. Firstly, contrast-enhanced abdominal CT scanning could not be performed in the earthquake situation due to suspicion of acute renal failure associated with crush syndrome, however, these non-enhanced CT scans could still image the injury patterns as illustrated in the present study. Secondly, this university hospital was 92 kilometers away from the epicenter, which could cause selection bias in the sampling of patients. Despite the limitations, this study illustrates the features of abdominal crush injury in survivors using MDCT focusing on the predominant anatomic distributions, which may be helpful in better understanding abdominal crush injury resulting from another earthquake to provide effective treatments.

In conclusion, the high incidence of lumbar vertebral fractures occurring predominantly in the transverse process of two vertebrae among L1-3 vertebrae, and in injuries of abdominal wall soft tissue; and a relatively high incidence of retroperitoneal parenchymal injury predominantly in kidney compared to intraperitoneal parenchymal injury predominantly in liver, might be features of abdominal crush injuries in an earthquake. We hope that these features of abdominal crush injuries may be helpful for the treatment of survivors in similar future earthquakes.

COMMENTS

Background

In the 2008 Sichuan earthquake, some patients sustained abdominal trauma associated with crush injury. Computed tomography (CT) scanning of the abdomen is currently considered the gold standard for detecting intra- and retroperitoneal lesions in trauma patients. However, the CT features of crush abdominal trauma in an earthquake have not been reported in the literature in detail.

Research frontiers

Abdominal crush injuries resulting from the 2008 Sichuan earthquake shown on emergency non-enhanced multidetector CT (MDCT) images were reviewed focusing on the anatomic regions which included the lumbar vertebrae, abdominal wall soft tissue, retroperitoneum and intraperitoneal space; and the types of traumatic lesions.

Innovations and breakthroughs

A high incidence of abdominal wall soft tissue injuries and in fractures of lumbar vertebrae predominantly in the transverse process of two vertebrae among L1-3 vertebrae, and a relatively high incidence of retroperitoneal parenchymal injury predominantly in kidney compared to intraperitoneal parenchymal injury predominantly in liver may be features of abdominal crush injuries in an earthquake.

Applications

The features of abdominal crush injuries in the 2008 Sichuan earthquake would be helpful for better understanding and treatment planning of abdominal crush trauma survivors in similar future earthquakes.

Terminology

Emergency non-enhanced MDCT is a rapid and valuable procedure to demonstrate abdominal crush injuries in an earthquake in detail, and is helpful for clinicians to better understand the features of abdominal crush injuries.

Peer review

In this manuscript, the authors described the features of abdominal crush injuries in an earthquake, which is interesting.

REFERENCES

1 **Muckart DJ**, Thomson SR. Undetected injuries: a preventable cause of increased morbidity and mortality. *Am J Surg* 1991; **162**: 457-460
2 **Hamilton JD**, Kumaravel M, Censullo ML, Cohen AM, Kievlan DS, West OC. Multidetector CT evaluation of active extravasation in blunt abdominal and pelvic trauma patients. *Radiographics* 2008; **28**: 1603-1616
3 **Scaglione M**. The use of sonography versus computed tomography in the triage of blunt abdominal trauma: the European perspective. *Emerg Radiol* 2004; **10**: 296-298
4 **Yoshii H**, Sato M, Yamamoto S, Motegi M, Okusawa S, Kitano M, Nagashima A, Doi M, Takuma K, Kato K, Aikawa N. Usefulness and limitations of ultrasonography in the initial evaluation of blunt abdominal trauma. *J Trauma* 1998; **45**: 45-50; discussion 50-51
5 **Federle MP**. Computed tomography of blunt abdominal trauma. *Radiol Clin North Am* 1983; **21**: 461-475
6 **Federle MP**, Griffiths B, Minagi H, Jeffrey RB. Splenic trauma: evaluation with CT. *Radiology* 1987; **162**: 69-71
7 **Becker CD**, Mentha G, Terrier F. Blunt abdominal trauma in adults: role of CT in the diagnosis and management of visceral injuries. Part 1: liver and spleen. *Eur Radiol* 1998; **8**: 553-562
8 **Mirvis SE**, Shanmuganathan K. Trauma radiology: part I. Computerized tomographic imaging of abdominal trauma. *J Intensive Care Med* 1994; **9**: 151-163
9 **Dong ZH**, Yang ZG, Chen TW, Feng YC, Wang QL, Chu ZG. Spinal injuries in the Sichuan earthquake. *N Engl J Med* 2009; **361**: 636-637
10 **Dong ZH**, Yang ZG, Chen TW, Feng YC, Chu ZG, Yu JQ, Bai HL, Wang QL. Crush thoracic trauma in the massive Sichuan earthquake: evaluation with multidetector CT of 215 cases. *Radiology* 2010; **254**: 285-291
11 **Chen TW**, Yang ZG, Dong ZH, Chu ZG, Yao J, Wang QL. Pelvic crush fractures in survivors of the Sichuan earthquake evaluated by digital radiography and multidetector computed tomography. *Skeletal Radiol* 2010; **39**: 1117-1122
12 **Chen TW**, Yang ZG, Wang QL, Dong ZH, Yu JQ, Zhuang ZP, Hou CL, Li ZL. Crush extremity fractures associated with the 2008 Sichuan earthquake: anatomic sites, numbers and statuses evaluated with digital radiography and multidetector computed tomography. *Skeletal Radiol* 2009; **38**: 1089-1097
13 **Peek-Asa C**, Kraus JF, Bourque LB, Vimalachandra D, Yu J, Abrams J. Fatal and hospitalized injuries resulting from the 1994 Northridge earthquake. *Int J Epidemiol* 1998; **27**: 459-465
14 **Mahoney LE**, Reutershan TP. Catastrophic disasters and the design of disaster medical care systems. *Ann Emerg Med* 1987; **16**: 1085-1091
15 **Mulvey JM**, Awan SU, Qadri AA, Maqsood MA. Profile of injuries arising from the 2005 Kashmir earthquake: the first 72 h. *Injury* 2008; **39**: 554-560
16 **Hessmann MH**, Hofmann A, Kreitner KF, Lott C, Rommens PM. The benefit of multislice CT in the emergency room management of polytraumatized patients. *Acta Chir Belg* 2006; **106**: 500-507
17 **Chen TW**, Yang ZG, Dong ZH, Chu ZG, Tang SS, Deng W. Earthquake-related crush injury versus non-earthquake injury in abdominal trauma patients on emergency multidetector computed tomography: a comparative study. *J Korean Med Sci* 2011; **26**: 438-443
18 **Sever MS**, Erek E, Vanholder R, Akoglu E, Yavuz M, Ergin H, Turkmen F, Korular D, Yenicesu M, Erbilgin D, Hoeben H, Lameire N. Clinical findings in the renal victims of a catastrophic disaster: the Marmara earthquake. *Nephrol Dial Transplant* 2002; **17**: 1942-1949
19 **Ersoy A**, Yavuz M, Usta M, Ercan I, Aslanhan I, Güllülü M, Kurt E, Emir G, Dilek K, Yurtkuran M. Survival analysis of the factors affecting in mortality in injured patients requiring dialysis due to acute renal failure during the Marmara earthquake: survivors vs non-survivors. *Clin Nephrol* 2003; **59**: 334-340

S- Editor Cheng JX **L- Editor** Webster JR **E- Editor** Zheng XM

World Journal of Radiology

Online Submissions: http://www.wjgnet.com/1949-8470office
wjr@wjgnet.com
doi:10.4329/wjr.v3.i5.141

World J Radiol 2011 May 28; 3(5): 141-146
ISSN 1949-8470 (online)

Era of diagnostic and interventional ultrasound

Hui-Xiong Xu

Hui-Xiong Xu, Department of Medical Ultrasound, Shanghai Tenth People's Hospital and the Tenth People's Hospital of Tongji University, Shanghai 200072, China
Author contributions: Xu HX solely contributed to this article.
Supported by (in part) Grant No. NCET-06-0723 from the Chinese Ministry of Education
Correspondence to: Hui-Xiong Xu, MD, PhD, Professor and Chair, Department of Medical Ultrasound, Shanghai Tenth People's Hospital and The Tenth People's Hospital of Tongji University, 301 Yanchangzhong Rd, Shanghai 200072, China. xuhuixiong@hotmail.com
Telephone: +86-21-66301031 Fax: +86-21-66301031
Received: March 2, 2011 Revised: March 19, 2011
Accepted: March 25, 2011
Published online: May 28, 2011

Abstract

It is an era of diagnostic and interventional ultrasound (US). Various new techniques such as three-dimensional US (3D US), interventional US, and contrast-enhanced US (CEUS) have been introduced into clinical practice. Dr. Xu and his colleagues have taken advantage of these techniques and carried out a series of relevant studies. Their use of 3D US in the liver, gallbladder, liver tumor volumetry, guidance for ablation, and 3D CEUS has widened the application of 3D US in the clinic. They found that prognosis in patients with hepatocellular carcinoma (HCC) after thermal ablation with curative intent was determined by treatment response to ablation, pretreatment serum AFP, and liver function reserve. Tumor response to treatment was the most predictive factor for long-term survival. They compared the use of percutaneous microwave ablation and radiofrequency ablation for the treatment of HCC and found that both are effective methods in treating HCCs. The local tumor control, complications related to treatment, and long-term survival were equivalent for the two modalities. They first compared the enhancement patterns of HCC and intrahepatic cholangiocarcinoma (ICC) and proposed the diagnostic clues for ICC, liver angiomyolipoma (AML), gallbladder cancer, renal carcinoma, and renal AML, which have greatly enhanced the role of CEUS in the clinic. They also evaluated the diagnostic performance of CEUS in characterizing complex cystic focal liver lesions and the agreement between two investigators with different experience levels; and found that CEUS is especially useful for the young investigator. They assessed the effect of anti-angiogenic gene therapy for HCC treated by microbubble-enhanced US exposure and concluded that gene therapy mediated by US exposure enhanced by a microbubble contrast agent may become a new treatment option for HCC.

Key words: Ablation; Cancer; Contrast-enhanced ultrasound; Interventional ultrasound; Liver; Three-dimensional ultrasound

Peer reviewer: Vlastimil Válek, MD, CSc., MBA, Professor, Department of Radiology, University Hospital Brno and Medical Faculty, Masaryk University Brno, Jihlavska 20, 639 00 Brno, Czech

Xu HX. Era of diagnostic and interventional ultrasound. *World J Radiol* 2011; 3(5): 141-146 Available from: URL: http://www.wjgnet.com/1949-8470/full/v3/i5/141.htm DOI: http://dx.doi.org/10.4329/wjr.v3.i5.141

INTRODUCTION AND EDUCATIONAL EXPERIENCE

Professor Dr. Hui-Xiong Xu is the Chair of the Department of Medical Ultrasound and the Vice-Chair of the Medical Imaging Center, Shanghai Tenth People's Hospital and the Tenth People's Hospital of Tongji University, Shanghai, China. He was enrolled in Tongji Medical University, Wuhan, China, in 1989 and obtained his M.D. degree in 1994. After graduation, he became a resident in the Department of Ultrasound, Tongji Hospital, Tongji Medical University and from then on he has devoted his career to the research and application of ultrasound (US) in medicine. In 1996, he became a doctoral student

of Professor Qing-Ping Zhang, a famous pioneer in Diagnostic Ultrasound. He learned a lot from Professor Zhang, not only the knowledge of specialty, but also how to be a righteous person. In 2000, his article entitled "3D Ultrasound of Abdominal Structures" was awarded The Grand Prix of The First 3D Clinical Contest, which was sponsored by the 3D Ultrasound Research Foundation in Korea. After 5-year doctoral course, he finished his thesis on Three-dimensional Ultrasound in Abdomen and obtained a PhD degree in Medical Imaging from Tongji Medical College, Huazhong University of Science and Technology, Wuhan, China. To further strengthen his academic background, he continued to seek strict scientific training and found a postdoctoral position in The First Affiliated Hospital, Sun Yat-Sen University, Guangzhou, China, under the instruction of Professor Ming-De Lu. In 2003, he became an Associate Professor and in 2006 a Professor of Sun Yat-Sen University through a non-routine promotion due to his significant academic achievements. In 2005, he visited the Department of Gastroenterology and Hepatology of Tokyo Medical University Hospital, Tokyo, Japan. He stayed there for 1 year to carry out research on contrast-enhanced US (CEUS) under the instruction of Professor Moriyasu as a Visiting Research Fellow. In 2011, he transferred to his current position. His academic positions are as follows: Supervisor of PhD candidates; Vice-president, Youth Committee of Ultrasound Branch, Chinese Medical Association (CMA); Member of Abdominal Group, Ultrasound Branch of CMA; Council Member of Abdominal Branch, Chinese Association of Ultrasound and Medical Engineering (CAUME); Member of Standing Council, Interventional Ultrasound Committee, Chinese Association of Medical Imaging Technique; Secretary-General, Member of Standing Committee of Ultrasound Branch, Guangdong Medical Doctor Association; Member of Standing Committee of Ultrasound Branch, Guangdong Association of Liver Diseases; Corresponding Member, European Society of Radiology; Member, International Contrast Ultrasound Society. He is the expert panel member for the new international liver CEUS guideline sponsored by the World Federation of Ultrasound in Medicine and Biology (WFUMB) and the American Institute of Ultrasound in Medicine, which will be released in August 2011 in Vienna, Austria. He serves as an editorial board member of a number of journals including the *Chinese Journal of Cancer*, *Chinese Journal of Medical Imaging Technique*, *Journal of US-China Medical Science*, and he is proud to be the Vice Editor-in-Chief of *World Journal of Radiology*. He is also a peer reviewer for journals such as *European Radiology* and *Journal of Ultrasound in Medicine*. In recent years, he has published approximately 30 articles in international journals as the first or corresponding author in the field of diagnostic and interventional US. Because of his outstanding achievements, he was named as the New Century Excellent Talent sponsored by the Chinese Ministry of Education and Distinguished Scholar by CAUME.

ACADEMIC STRATEGIES AND GOALS

In recent years, Dr. Xu's research areas focused on three-dimensional US (3D US), CEUS, and interventional US. Besides the use of 3D US in prenatal diagnosis, he also utilized 3D US to visualize the liver and gallbladder, guide interventional procedures, and evaluate treatment response after local therapies. Since the introduction of CEUS in China in 2004, he has carried out a number of studies to evaluate its usefulness in clinical practice. He first reported the use of CEUS in small focal liver lesions by using the new generation contrast agent SonoVue and novel low mechanical index contrast specific techniques, as well as the enhancement pattern of intrahepatic cholangiocarcinoma (ICC). Due to his contribution concerning the use of CEUS in liver, he was invited by Professor Claudon, the Chairman of WFUMB, to compile the new version of the International CEUS Guideline for Liver. His career goal is to utilize up-to-date US techniques to improve the diagnosis and treatment of various diseases.

ACADEMIC ACHIEVEMENTS

Dr. Xu's activities in diagnostic and interventional US and his contributions are as follows:

3D US

Xu *et al*[1] assessed the differences between 2D and 3D US in evaluating fetal malformations. The results showed that in comparison with 2D US, 3D US improves the diagnostic capability by offering more diagnostic information in evaluating fetal malformations, particularly in displaying malformations of the cranium and face, spine and extremities, and body surface. 3D US is a valuable adjunct to 2D US in prenatal diagnosis. They investigated the potential clinical usefulness of 3D gray scale volume rendering in the liver. That is a challenging task since few investigators had previously evaluated this. They found that in patients with ascites, 3D US was superior to 2D US in terms of surface features, edges, overall 3D impression, image clarity, and structural relationships. In patients without ascites, 3D US was superior to 2D US with respect to the continuity of intrahepatic vessels, overall 3D impression of the vessels, image clarity, and the relationship between lesions and neighboring vessels[2]. They first evaluated the accuracy and reproducibility of a commercially-available 3D US volume measurement system based on automatic border detection technique, VOCAL™ (virtual organ computer-aided analysis) in the volumetry of liver tumors. They confirmed that the new system can greatly reduce the time taken and manual labor needed for volume measurement with high accuracy and reproducibility. 3D US volumetry using the new system is more acceptable and valuable in clinical practice and is expected to be useful for evaluation of the efficacy of tumor therapy *in situ* in patients with hepatic tumors[3]. They also found that a 3D power Doppler projection image gives a better overall picture of vascular distribution

than a 2D slice and significantly correlates with angiography for delineating vascularity in hepatocellular carcinoma (HCC)[4]. The gallbladder is an idea organ for 3D US, Xu *et al*[5] compared 3D US with 2D US for the diagnosis of gallbladder diseases. It was found that 3D US adds no advantages for the diagnosis of gallstones compared with 2D US, but it is better than 2D US for differential diagnosis of gallbladder polyps and may improve the localization and staging for gallbladder carcinoma. Their efforts have widened the utility of 3D US in clinical practice.

Interventional US

US-guided ablation therapy for HCC has gained increased attention as a curative option for early HCC. Xu *et al*[6] investigated the therapeutic efficacy of thermal ablation for the treatment of HCC using microwave and radiofrequency (RF) energy application. Complete ablation was obtained in 92.6% (176/190) nodules and local recurrence was found in 9.5% nodules in the follow-up. 1, 2 and 3-year cumulative survival was 75.6, 58.5, and 50.0%, respectively. The relatively low survival rates were partly due to the fact that recurrent HCC accounted for the majority of the cases. They also tried to identify prognostic factors for long-term outcome in patients with HCC after percutaneous microwave or radiofrequency ablation[7]. Prognosis for patients with HCC after thermal ablation with curative intent was determined by treatment response to ablation, pretreatment serum AFP, and liver function reserve. Tumor response to treatment was the most predictive factor for long-term survival and was related to tumor size, thus careful selection of patients for ablation therapy is recommended. They compared the use of percutaneous microwave ablation and radiofrequency ablation for the treatment of HCC and found that percutaneous microwave ablation and radiofrequency ablation are both effective methods in treating HCCs. The local tumor control, complications related to treatment, and long-term survival were equivalent for the two modalities[8,9]. To improve the targeting and monitoring of ablation, they applied 3D US in the guidance. Their results showed that 3D US was useful in delineation of expandable RF electrodes, improvement of operator confidence level, determination of applicator placement, and visualization of the position relationship between the applicator and adjacent critical structures during procedures of liver cancer ablation under image guidance[10]. Tumor location close to the diaphragm or gastrointestinal tract was regarded as a treatment contraindication due to poor visibility of the tumor or increased risk of thermal injury to the adjacent organs. To solve this problem, Xu *et al*[11] utilized artificial pleural effusion or ascites to improve visualization of the tumor and isolation from adjacent critical structures. The technical success rates were 95% for artificial pleural effusion and 100% for artificial ascites. These techniques are safe and effective, which provide treatment opportunities for complicated cases. To improve the treatment response evaluation after ablation therapy, Xu *et al*[12] investigated the potential usefulness of 3D CEUS for this purpose. They found that 3D CEUS enhances the diagnostic confidence in the majority of patients and even changes the management in some patients. 3D CEUS has potential usefulness in evaluating treatment response in liver cancer after local therapies.

CEUS

Low mechanical index CEUS has greatly changed the status of US techniques since its introduction into clinic practice.

Liver: Xu *et al*[13] evaluated its performance in diagnosing focal liver lesions. Their results showed that the sensitivity, specificity, and positive predictive value, respectively, were 88.8%, 89.2%, and 91.3% for HCC; 81%, 100%, and 100% for liver metastasis; 57.1%, 100%, and 100% for ICC; 94.6%, 100%, and 100% for liver hemangioma; and 90.9%, 97.8%, and 71.4% for focal nodular hyperplasia. Xu *et al*[14] further assessed the diagnostic performance of CEUS characterization of small focal liver lesions (FLLs; ≤ 3.0 cm in diameter). Their results showed that after review of CEUS, ROC analysis revealed a significant improvement in differentiating between malignant and benign small FLLs, where the areas under the ROC curve were 0.856 at baseline US *vs* 0.954 at CEUS ($P < 0.001$) and 0.857 *vs* 0.954 for reader 2 ($P = 0.003$). The sensitivity, negative predictive value, and accuracy for both readers also improved significantly after contrast agent administration (all $P < 0.001$). A better result of specific diagnosis was obtained [38.5% (77/200) at baseline US *vs* 80.5% (161/200) at CEUS for reader 1 and 34.5% (69/200) *vs* 80.5% (161/200) for reader 2; both $P < 0.001$] after contrast agent administration, and a better interobserver agreement was achieved ($\kappa = 0.425$ at baseline US *vs* 0.716 at CEUS). Thus, CEUS improves the diagnostic performance in small FLLs compared with baseline US. For smaller FLLs (≤ 2 cm), similar results were obtained although the sensitivity for HCC was relatively low[15].

ICC is a malignant tumor originating from the bile duct epithelium of the interlobular biliary duct. US findings are nonspecific for ICC. Xu *et al*[16] and Chen *et al*[17,18] evaluated the use of CEUS in characterization of ICC. They first reported that four enhancement patterns exist in the arterial phase for ICC, which were (1) peripheral irregular rim-like hyperenhancement; (2) diffuse heterogeneous hyperenhancement; (3) diffuse homogeneous hyperenhancement; and (4) diffuse heterogeneous hypoenhancement, which accounts for 47.5%, 22.5%, 12.5% and 17.5%, respectively, for ICC[17]. The enhancement patterns of ICC on CEUS were consistent with those on contrast-enhanced CT (CECT) in the arterial phase, whereas in the portal phase ICC faded out more obviously on CEUS than on CECT. CEUS had the same accuracy as CECT in diagnosing ICCs, and so can be used as a new modality for the characterization of ICC. Concerning the differentiation between ICC and HCC, the sensitivity (28%-44% *vs* 82%-90%) and accuracy

(64%-71% *vs* 90%) improved significantly after CEUS (all $P < 0.05$). The interobserver agreement increased from $\kappa = 0.575$ at BUS to $\kappa = 0.720$ after CEUS[18]. Thus CEUS significantly improves the diagnostic performance in the differentiation between ICC and HCC.

Complex cystic FLLs are those containing large fluid-filled areas within the lesions; they are increasingly common in clinical practice as a result of the increasing use of hepatic imaging. Lin *et al*[19] evaluated the diagnostic performance of CEUS in characterizing complex cystic FLLs. The US and CEUS images were reviewed by a resident radiologist and a staff radiologist independently. After ROC analysis, the areas (Az) under the ROC curve were 0.774 at US *vs* 0.922 at CEUS ($P = 0.047$) by the resident radiologist, and 0.917 *vs* 0.935 ($P = 0.38$) by the staff radiologist. A significant difference in Az between the resident and the staff radiologist was found for US (0.774 *vs* 0.917, $P = 0.044$), but not for CEUS (0.922 *vs* 0.935, $P = 0.42$). Interobserver agreement was improved after CEUS ($\kappa = 0.325$ at US *vs* $\kappa = 0.774$ at CEUS). Real-time CEUS improves the capability of discriminating between benign and malignant complex cystic FLLs, especially for the resident radiologist.

Hepatic angiomyolipoma (AML) is generally considered a rare benign mesenchymal tumor of the liver. With the increasing clinical application of imaging, more and more hepatic AMLs are being detected. Wang *et al*[20] found that arterial hyperenhancement and subsequent sustained enhancement on CEUS were found in the majority of hepatic AMLs. The combination of BUS and CEUS leads to the correct diagnosis in the majority of hepatic AMLs, and is higher than the success rate achieved by BUS alone. For those unusual benign FLLs, Xu *et al*[21] found that CEUS was beneficial in leading to a benign diagnosis for some lesions showing hyperenhancement during the arterial phase and sustained enhancement during the portal or late phase, such as liver AML and lipoma. The benign nature of other lesions showing no enhancement during all phases, such as solitary necrotic nodules and focal fibrosis, was also observable. On the other hand, for those lesions showing hyperenhancement, isoenhancement, or hypoenhancement during the arterial phase and hypoenhancement during the late phase, including intrahepatic biliary cystadenoma, biliary epithelial dysplasia, infected liver diseases, inflammatory pseudotumor, sarcoidosis, and peliosis hepatis, the differential diagnosis between benignity and malignancy was difficult, and pathologic tests were mandatory.

The feasibility of 3D CEUS in liver imaging was evaluated by Xu *et al*[22]. The patients were classified into two groups: those for characterization and those for local treatment response evaluation. The investigators found that 3D CEUS results in better image quality and leads to higher diagnostic confidence in those for treatment response evaluation, and perhaps is more useful in this aspect in future clinical setting.

Gallbladder and bile duct: Conventional gray-scale US is the first-line imaging investigation for diagnosis of gallbladder diseases, but can result in difficulty in determining the nature of the gallbladder lesions in some cases, especially in differentiating chronic cholecystitis with thickened wall from gallbladder carcinoma with thickened wall or in differentiating motionless sludge from gallbladder cancer[23,24]. Xie *et al*[23] evaluated the usefulness of CEUS in diagnosing gallbladder diseases. They found that characters such as hyperenhancement or isoenhancement in the early phase and then fading out to hypoenhancement, as well as destruction of the gallbladder wall intactness, are more frequent in malignancy. Conventional US resulted in correct original diagnoses in 68.8% patients, and CEUS in 96.3%. Thus, CEUS is useful in the differential diagnosis between malignant and benign gallbladder diseases.

Xu *et al*[25] compared the enhancement pattern of hilar cholangiocarcinoma on CEUS with that on CECT. They found that the enhancement pattern of hilar cholangiocarcinoma on CEUS was similar with that on CECT in the arterial phase, whereas in the portal phase, hilar cholangiocarcinoma shows hypoenhancement on CEUS. CEUS and CECT lead to similar results in evaluating portal vein infiltration and diagnosis of this entity.

Xu *et al*[26] first reported the experience of CEUS in villous adenoma of the extrahepatic bile duct. In this disease, CEUS showed hyperenhancement during the arterial phase and subsequent washout, suggesting it was a hypervascular lesion and excluded the diagnosis of sludge, nonshadowing stones, and blood clots. Because the lesion exhibited homogeneous echogenicity, the bile duct wall was intact, and invasive signs were absent on a BUS, the diagnosis of a benign tumor such as an adenoma was suggested.

Kidney: Renal cell cancer (RCC) is the most common malignant tumor of kidney, which accounts for 80% to 90% of renal tumors. Xu *et al*[27] observed the CEUS features of RCC and found that hyper- or iso-enhancement during the cortical phase, subsequent washout in the late phase, inhomogeneous enhancement, and perilesional rim-like enhancement are clues for RCCs, which might be useful for characterization of RCCs. They[28] further evaluated the usefulness of CEUS in differentiating RCC from renal AML (RAML). They found that the CEUS features of early wash-out, heterogeneous enhancement, and an enhanced peritumoral rim are highly suggestive of RCC, whereas homogeneous enhancement and prolonged enhancement are characteristic manifestations of RAML. The sensitivity, specificity, positive predictive value, negative predictive value, and accuracy of CEUS in differentiation were 88.2%, 97.0%, 98.8%, 74.4%, and 90.5%, respectively. Thus, CEUS is valuable in differentiating RCC from RAML.

Experimental study: Nie *et al*[29] explored the effects of US exposure combined with microbubble contrast agent (SonoVue) on the permeability of the cellular membrane

and on the expression of plasmid DNA encoding enhanced green fluorescent protein (pEGFP) transfer into human umbilical vein endothelial cells (HUVECs). They found that the percentage of FD500-positive HUVECs in the group of US exposure combined with SonoVue was significantly higher than that of the group of US exposure alone (66.6% ± 4.1% *vs* 24.0% ± 5.5%, $P < 0.001$). Compared with the group of US exposure alone, the transfection expression rate of pEGFP in HUVECs was markedly increased with the addition of SonoVue (1.5% ± 0.2% *vs* 16.1% ± 1.9%, $P < 0.001$). No statistically significant difference was observed in the survival rates of the HUVECs between the US group with and without the addition of SonoVue (94.1% ± 2.3% *vs* 91.1% ± 4.1%). The cell membrane permeability of HUVECs and the transfection efficiency of pEGFP into HUVECs exposed to US are significantly increased after addition of an US contrast agent without obvious damage to the survival of HUVECs. This noninvasive gene transfer method may be a useful tool for clinical gene therapy.

They further assessed the effect of anti-angiogenic gene therapy for HCC treated by microbubble-enhanced US exposure[30]. Compared with the group treated by US alone, KDR-tk gene treatment by US combined with SonoVue inhibited tumor growth and increased survival time of tumor-bearing mice; microvessel density in the US and SonoVue group was significantly lower than that in the US alone group (12.3 ± 1.4 *vs* 27.4 ± 3.2, $P < 0.05$). An apoptosis index increased in the group treated with US and SonoVue compared with the group treated with US alone (25 ± 3.6 *vs* 36 ± 3.8, $P < 0.05$), whereas there was no significant difference between the SonoVue alone group and the phosphate-buffered saline alone group (17 ± 1.8 *vs* 14 ± 1.2, $P > 0.05$). The authors concluded that gene therapy mediated by US exposure enhanced by a microbubble contrast agent may become a new treatment option for persistent HCC.

CONCLUSION

Due to the rapid progress in image processing and transducer design, US has gained increasing attention in clinical practice in recent years. It is now an era of diagnostic and interventional US[31-33]. Dr. Xu's studies in the fields of 3D US, interventional US, and CEUS has greatly enriched the use of US in diagnosis and treatment.

ACKNOWLEDGMENTS

I am grateful to Professor Qing-Ping Zhang for bringing me to the world of US, to Professor Ming-De Lu for giving me numerous chances to learn and practice, and to Prof. Moriyasu F for opening a new window of US to me. I would also express my gratitude to my colleagues worldwide for their kind collaboration.

REFERENCES

1 **Xu HX**, Zhang QP, Lu MD, Xiao XT. Comparison of two-dimensional and three-dimensional sonography in evaluating fetal malformations. *J Clin Ultrasound* 2002; **30**: 515-525
2 **Xu HX**, Lu MD, Zhou YQ, Zhang QP, Yin XY, Xie XY, Liu L. Three-dimensional gray scale volume rendering of the liver: preliminary clinical experience. *J Ultrasound Med* 2002; **21**: 961-970
3 **Xu HX**, Yin XY, Lu MD, Liu GJ, Xu ZF. Estimation of liver tumor volume using a three-dimensional ultrasound volumetric system. *Ultrasound Med Biol* 2003; **29**: 839-846
4 **Xu HX**, Liu L, Lu MD, Li HP, Liu GJ, Li JP. Three-dimensional power Doppler imaging in depicting vascularity in hepatocellular carcinoma. *J Ultrasound Med* 2003; **22**: 1147-1154
5 **Xu HX**, Yin XY, Lu MD, Liu L, Yue DC, Liu GJ. Comparison of three- and two-dimensional sonography in diagnosis of gallbladder diseases: preliminary experience. *J Ultrasound Med* 2003; **22**: 181-191
6 **Xu HX**, Xie XY, Lu MD, Chen JW, Yin XY, Xu ZF, Liu GJ. Ultrasound-guided percutaneous thermal ablation of hepatocellular carcinoma using microwave and radiofrequency ablation. *Clin Radiol* 2004; **59**: 53-61
7 **Xu HX**, Lu MD, Xie XY, Yin XY, Kuang M, Chen JW, Xu ZF, Liu GJ. Prognostic factors for long-term outcome after percutaneous thermal ablation for hepatocellular carcinoma: a survival analysis of 137 consecutive patients. *Clin Radiol* 2005; **60**: 1018-1025
8 **Lu MD**, Xu HX, Xie XY, Yin XY, Chen JW, Kuang M, Xu ZF, Liu GJ, Zheng YL. Percutaneous microwave and radiofrequency ablation for hepatocellular carcinoma: a retrospective comparative study. *J Gastroenterol* 2005; **40**: 1054-1060
9 **Ohmoto K**, Yamamoto S. Comparison between radiofrequency ablation and percutaneous microwave coagulation therapy for small hepatocellular carcinomas. *Clin Radiol* 2006; **61**: 800-801; author reply 801-802
10 **Xu HX**, Yin XY, Lu MD, Xie XY, Xu ZF, Liu GJ. Usefulness of three-dimensional sonography in procedures of ablation for liver cancers: initial experience. *J Ultrasound Med* 2003; **22**: 1239-1247
11 **Liu LN**, Xu HX, Lu MD, Xie XY. Percutaneous ultrasound-guided thermal ablation for liver tumor with artificial pleural effusion or ascites. *Chin J Cancer* 2010; **29**: 830-835
12 **Xu HX**, Lu MD, Xie XH, Xie XY, Kuang M, Xu ZF, Liu GJ, Wang Z, Chen LD, Lin MX. Treatment response evaluation with three-dimensional contrast-enhanced ultrasound for liver cancer after local therapies. *Eur J Radiol* 2010; **76**: 81-88
13 **Xu HX**, Liu GJ, Lu MD, Xie XY, Xu ZF, Zheng YL, Liang JY. Characterization of focal liver lesions using contrast-enhanced sonography with a low mechanical index mode and a sulfur hexafluoride-filled microbubble contrast agent. *J Clin Ultrasound* 2006; **34**: 261-272
14 **Xu HX**, Liu GJ, Lu MD, Xie XY, Xu ZF, Zheng YL, Liang JY. Characterization of small focal liver lesions using real-time contrast-enhanced sonography: diagnostic performance analysis in 200 patients. *J Ultrasound Med* 2006; **25**: 349-361
15 **Xu HX**, Xie XY, Lu MD, Liu GJ, Xu ZF, Zheng YL, Liang JY, Chen LD. Contrast-enhanced sonography in the diagnosis of small hepatocellular carcinoma < or =2 cm. *J Clin Ultrasound* 2008; **36**: 257-266
16 **Xu HX**, Lu MD, Liu GJ, Xie XY, Xu ZF, Zheng YL, Liang JY. Imaging of peripheral cholangiocarcinoma with low-mechanical index contrast-enhanced sonography and SonoVue: initial experience. *J Ultrasound Med* 2006; **25**: 23-33
17 **Chen LD**, Xu HX, Xie XY, Lu MD, Xu ZF, Liu GJ, Liang JY, Lin MX. Enhancement patterns of intrahepatic cholangiocarcinoma: comparison between contrast-enhanced ultrasound and contrast-enhanced CT. *Br J Radiol* 2008; **81**: 881-889
18 **Chen LD**, Xu HX, Xie XY, Xie XH, Xu ZF, Liu GJ, Wang Z, Lin MX, Lu MD. Intrahepatic cholangiocarcinoma and hepatocellular carcinoma: differential diagnosis with contrast-enhanced ultrasound. *Eur Radiol* 2010; **20**: 743-753
19 **Lin MX**, Xu HX, Lu MD, Xie XY, Chen LD, Xu ZF, Liu

GJ, Xie XH, Liang JY, Wang Z. Diagnostic performance of contrast-enhanced ultrasound for complex cystic focal liver lesions: blinded reader study. *Eur Radiol* 2009; **19**: 358-369
20 **Wang Z**, Xu HX, Xie XY, Xie XH, Kuang M, Xu ZF, Liu GJ, Chen LD, Lin MX, Lu MD. Imaging features of hepatic angiomyolipomas on real-time contrast-enhanced ultrasound. *Br J Radiol* 2010; **83**: 411-418
21 **Xu HX**, Xie XY, Lu MD, Liu GJ, Xu ZF, Liang JY, Chen LD. Unusual benign focal liver lesions: findings on real-time contrast-enhanced sonography. *J Ultrasound Med* 2008; **27**: 243-254
22 **Xu HX**, Lu MD, Xie XH, Xie XY, Xu ZF, Chen LD, Liu GJ, Liang JY, Lin MX, Wang Z, Huang B. Three-dimensional contrast-enhanced ultrasound of the liver: experience of 92 cases. *Ultrasonics* 2009; **49**: 377-385
23 **Xie XH**, Xu HX, Xie XY, Lu MD, Kuang M, Xu ZF, Liu GJ, Wang Z, Liang JY, Chen LD, Lin MX. Differential diagnosis between benign and malignant gallbladder diseases with real-time contrast-enhanced ultrasound. *Eur Radiol* 2010; **20**: 239-248
24 **Xu HX**. Contrast-enhanced ultrasound in the biliary system: Potential uses and indications. *World J Radiol* 2009; **1**: 37-44
25 **Xu HX**, Chen LD, Xie XY, Xie XH, Xu ZF, Liu GJ, Lin MX, Wang Z, Lu MD. Enhancement pattern of hilar cholangiocarcinoma: contrast-enhanced ultrasound versus contrast-enhanced computed tomography. *Eur J Radiol* 2010; **75**: 197-202
26 **Xu HX**, Chen LD. Villous adenoma of extrahepatic bile duct: contrast-enhanced sonography findings. *J Clin Ultrasound* 2008; **36**: 39-41
27 **Xu ZF**, Xu HX, Xie XY, Liu GJ, Zheng YL, Liang JY, Lu MD. Renal cell carcinoma: real-time contrast-enhanced ultrasound findings. *Abdom Imaging* 2010; **35**: 750-756
28 **Xu ZF**, Xu HX, Xie XY, Liu GJ, Zheng YL, Lu MD. Renal cell carcinoma and renal angiomyolipoma: differential diagnosis with real-time contrast-enhanced ultrasonography. *J Ultrasound Med* 2010; **29**: 709-717
29 **Nie F**, Xu HX, Tang Q, Lu MD. Microbubble-enhanced ultrasound exposure improves gene transfer in vascular endothelial cells. *World J Gastroenterol* 2006; **12**: 7508-7513
30 **Nie F**, Xu HX, Lu MD, Wang Y, Tang Q. Anti-angiogenic gene therapy for hepatocellular carcinoma mediated by microbubble-enhanced ultrasound exposure: an in vivo experimental study. *J Drug Target* 2008; **16**: 389-395
31 **Xu HX**. Contrast-enhanced ultrasound: The evolving applications. *World J Radiol* 2009; **1**: 15-24
32 **Wong GL**, Xu HX, Xie XY. Detection of focal liver lesions in cirrhotic liver using contrast-enhanced ultrasound. *World J Radiol* 2009; **1**: 25-36
33 **Xu HX**, Lu MD. The current status of contrast-enhanced ultrasound in China. *J Med Ultrasonics* 2010; **37**: 97-106

S- Editor Cheng JX **L- Editor** Webster JR **E- Editor** Zheng XM

World Journal of Radiology

Online Submissions: http://www.wjgnet.com/1949-8470office
wjr@wjgnet.com
www.wjgnet.com

World J Radiol 2011 May 28; 3(5): I
ISSN 1949-8470 (online)

Acknowledgments to reviewers of *World Journal of Radiology*

Many reviewers have contributed their expertise and time to the peer review, a critical process to ensure the quality of *World Journal of Radiology*. The editors and authors of the articles submitted to the journal are grateful to the following reviewers for evaluating the articles (including those published in this issue and those rejected for this issue) during the last editing time period.

Charles Bellows, MD, Associate Professor, Chief of General Surgery, Tulane University, Department of Surgery SL-22, 1430 Tulane Ave, New Orleans, LA 70112, United States

Filippo Cademartiri, MD, PhD, Departmento of Radiology - c/o Piastra Tecnica - Piano 0, Azienda Ospedaliero-Universitaria di Parma, Via Gramsci, 14 - 43100 Parma, Italy

Sergio Casciaro, PhD, Institute of Clinical Physiology - National Research Council,Campus Universitario Ecotekne, Via Monteroni, 73100 Lecce, Italy

Chan Kyo Kim, MD, Assistant Professor, Department of Radiology, Samsung Medical Center, Sungkyunkwan University School of Medicine, 50 Ilwon-dong, Kangnam-gu, Seoul 135-710, South Korea

Stefania Romano, MD, A. Cardarelli Hospital, Department of Diagnostic Imaging, Section of General and Emergency Radiology, Viale Cardarelli, 9, 80131 Naples, Italy

Francesco Lassandro, MD, Department of Radiology, Monaldi Hospital, via Leonardo Bianchi, Napoli, 80129, Italy

Kennith F Layton, MD, FAHA, Division of Neuroradiology and Director of Interventional Neuroradiology, Department of Radiology, Baylor University Medical Center, 3500 Gaston Avenue, Dallas, TX 75246, United States

Yicheng Ni, MD, PhD, Professor, Biomedical Imaging, Interventional Therapy and Contrast Media Research, Department of Radiology, University Hospitals, K.U. Leuven, Herestraat 49, B-3000, Leuven, Belgium

Yi-Xiang Wang, MMed, PhD, Associate Professor, Department of Diagnostic Radiology and Organ Imaging, Prince of Wales Hospital, The Chinese University of Hong Kong, Shatin, NT, Hong Kong, China

Ying Xiao, PhD, Professor, Director, Medical Physics, Department of Radiation Oncology, Thomas Jefferson University Hospital, Philadelphia, PA 19107-5097, United States

WJR World Journal of Radiology

Online Submissions: http://www.wjgnet.com/1949-8470office
wjr@wjgnet.com
www.wjgnet.com

World J Radiol 2011 May 28; 3(5): I
ISSN 1949-8470 (online)

Events Calendar 2011

January 23-27
Radiology at Snowbird
San Diego, Mexico

January 24-28
Neuro/ENT at the Beach
Palm Beach, FL, United States

February 28-29
MIAD 2011 - 2nd International Workshop on Medical Image Analysis and Description for Diagnosis System
Rome, Italy

February 5-6
Washington Neuroradiology Review
Arlington, VA, United States

February 12-17
MI11 - SPIE Medical Imaging 2011
Lake Buena Vista, FL, United States

February 17-18
2nd National Conference Diagnostic and Interventional Radiology 2011
London, United Kingdom

Februrary 17-18
VII National Neuroradiology Course
Lleida, Spain

February 18
Radiology in child protection
Nottingham, United Kingdom

Februrary 19-22
COMPREHENSIVE REVIEW OF MUSCULOSKELETAL MRI
Lake Buena Vista, FL, United States

March 2-5
2011 Abdominal Radiology Course
Carlsbad, CA, United States

March 3-7
European Congress of Radiology Meeting ECR 2011 Vienna, Austria

March 6-9
World Congress Thoracic Imaging - IV
Bonita Springs, FL, United States

March 14-18
9th Annual NYU Radiology Alpine Imaging Symposium at Beaver Creek
Beaver Creek, CO, United States

March 20-25
Abdominal Radiology Course 2011
Carlsbad, CA, United States

March 26-31
2011 SIR Annual Meeting
Chicago, IL, United States

March 28-April 1
University of Utah Neuroradiology 2nd Intensive Interactive Brain & Spine Imaging Conference
Salt Lake City, UT, United States

April 3-8
1st Annual Ottawa Radiology Resident Review
Ottawa, Canada

April 3-8
43rd International Diagnostic Course Davos on Diagnostic Imaging and Interventional Techniques
Davos, Switzerland

April 6-9
Image-Based Neurodiagnosis: Intensive Clinical and Radiologic Review, CAQ Preparation
Cincinnati, OH, United States

April 28-May 1
74th Annual Scientific Meeting of the Canadian Association of Radiologists CAR
Montreal, Canada

May 5-8
EMBL Conference-Sixth International Congress on Electron Tomography
Heidelberg, Germany

May 10-13
27th Iranian Congress of Radiology
Tehran, Iran

May 14-21
Radiology in Marrakech
Marrakech, Morocco

May 21-24
European Society of Gastrointestinal and Abdominal Radiology 2011 Annual Meeting
Venice, Italy

May 23-25
Sports Medicine Imaging State of the Art: A Collaborative Course for Radiologists and Sports Medicine Specialists
New York, NY, United States

May 24-26
Russian Congress of Radiology
Moscow, Russia

May 28-31
International Congress of Pediatric Radiology (IPR)
London, United Kingdom

June 4-8
58th Annual Meeting of the Society of Nuclear Medicine
San Antonio,
TX, United States

June 6-8
UKRC 2011 - UK Radiological Congress
Manchester, United Kingdom

June 8-11
CIRA 2011 - Canadian Internventinal Radiology Association Meeting
Montreal, QC, Canada

June 9-10
8th ESGAR Liver Imaging Workshop
Dublin, Ireland

June 17-19
ASCI 2011 - 5th Congress of Asian Society of Cardiovascular Imaging
Hong Kong, China

June 22-25
CARS 2011 - Computer Assisted Radiology and Surgery - 25th International Congress and Exhibition Berlin, Germany

June 27-July 1
NYU Summer Radiology Symposium at The Sagamore
Lake George, NY, United States

July 18-22
Clinical Case-Based Radiology Update in Iceland
Reykjavik, Iceland

August 1-5
NYU Clinical Imaging Symposium in Santa Fe
Santa Fe, NM, United States

September 22-25
European Society of Neuroradiology (ESNR) XXXV Congress and 19th Advanced Course
Antwerp, Belgium

October 12-14
International Conference Vipimage 2011 - Computational Vision and Medical Image Processing
Algarve, Portugal

October 15-16
Essentials of Emergency and Trauma Radiology
Ottawa, Canada

October 23-29
2011 IEEE NSS - 2011 IEEE Nuclear Science Symposium and Medical Imaging Conference
Valencia, Spain

October 25-28
NYU Radiology in Scottsdale - Fall Radiology Symposium in Scottsdale
Scottsdale, AZ,
United States

October 28-30
Fourth National Congress of Professionals of Radiological Techniques Florianópolis, Brazil

October 28-30
Multi-Modality Gynecological & Obstetric Imaging
Ottawa, Canada

November 3-4
9th ESGAR Liver Imaging Workshop
Taormina, Italy

November 15-19
EANM 2011 - Annual Congress of the European Association of Nuclear Medicine
Birmingham,
United Kingdom

November 22-29
NSS/MIC - Nuclear Science Symposium and Medical Imaging Conference 2011 Valencia, Spain

November 26-28
8th Asia Oceaninan Congress of Neuro-Radiology Bangkok,
Thailand

World Journal of Radiology

Online Submissions: http://www.wjgnet.com/1949-8470office
wjr@wjgnet.com
www.wjgnet.com

World J Radiol 2011 May 28; 3(5): I-V
ISSN 1949-8470 (online)

INSTRUCTIONS TO AUTHORS

GENERAL INFORMATION

World Journal of Radiology (*World J Radiol*, *WJR*, online ISSN 1949-8470, DOI: 10.4329), is a monthly, open-access (OA), peer-reviewed journal supported by an editorial board of 319 experts in Radiology from 40 countries.

The biggest advantage of the OA model is that it provides free, full-text articles in PDF and other formats for experts and the public without registration, which eliminates the obstacle that traditional journals possess and usually delays the speed of the propagation and communication of scientific research results. The open access model has been proven to be a true approach that may achieve the ultimate goal of the journals, i.e. the maximization of the value to the readers, authors and society.

Maximization of personal benefits

The role of academic journals is to exhibit the scientific levels of a country, a university, a center, a department, and even a scientist, and build an important bridge for communication between scientists and the public. As we all know, the significance of the publication of scientific articles lies not only in disseminating and communicating innovative scientific achievements and academic views, as well as promoting the application of scientific achievements, but also in formally recognizing the "priority" and "copyright" of innovative achievements published, as well as evaluating research performance and academic levels. So, to realize these desired attributes of *WJR* and create a well-recognized journal, the following four types of personal benefits should be maximized. The maximization of personal benefits refers to the pursuit of the maximum personal benefits in a well-considered optimal manner without violation of the laws, ethical rules and the benefits of others. (1) Maximization of the benefits of editorial board members: The primary task of editorial board members is to give a peer review of an unpublished scientific article via online office system to evaluate its innovativeness, scientific and practical values and determine whether it should be published or not. During peer review, editorial board members can also obtain cutting-edge information in that field at first hand. As leaders in their field, they have priority to be invited to write articles and publish commentary articles. We will put peer reviewers' names and affiliations along with the article they reviewed in the journal to acknowledge their contribution; (2) Maximization of the benefits of authors: Since *WJR* is an open-access journal, readers around the world can immediately download and read, free of charge, high-quality, peer-reviewed articles from *WJR* official website, thereby realizing the goals and significance of the communication between authors and peers as well as public reading; (3) Maximization of the benefits of readers: Readers can read or use, free of charge, high-quality peer-reviewed articles without any limits, and cite the arguments, viewpoints, concepts, theories, methods, results, conclusion or facts and data of pertinent literature so as to validate the innovativeness, scientific and practical values of their own research achievements, thus ensuring that their articles have novel arguments or viewpoints, solid evidence and correct conclusion; and (4) Maximization of the benefits of employees: It is an iron law that a first-class journal is unable to exist without first-class editors, and only first-class editors can create a first-class academic journal. We insist on strengthening our team cultivation and construction so that every employee, in an open, fair and transparent environment, could contribute their wisdom to edit and publish high-quality articles, thereby realizing the maximization of the personal benefits of editorial board members, authors and readers, and yielding the greatest social and economic benefits.

Aims and scope

The major task of *WJR* is to rapidly report the most recent improvement in the research of medical imaging and radiation therapy by the radiologists. *WJR* accepts papers on the following aspects related to radiology: Abdominal radiology, women health radiology, cardiovascular radiology, chest radiology, genitourinary radiology, neuroradiology, head and neck radiology, interventional radiology, musculoskeletal radiology, molecular imaging, pediatric radiology, experimental radiology, radiological technology, nuclear medicine, PACS and radiology informatics, and ultrasound. We also encourage papers that cover all other areas of radiology as well as basic research.

Columns

The columns in the issues of *WJR* will include: (1) Editorial: To introduce and comment on major advances and developments in the field; (2) Frontier: To review representative achievements, comment on the state of current research, and propose directions for future research; (3) Topic Highlight: This column consists of three formats, including (A) 10 invited review articles on a hot topic, (B) a commentary on common issues of this hot topic, and (C) a commentary on the 10 individual articles; (4) Observation: To update the development of old and new questions, highlight unsolved problems, and provide strategies on how to solve the questions; (5) Guidelines for Basic Research: To provide guidelines for basic research; (6) Guidelines for Clinical Practice: To provide guidelines for clinical diagnosis and treatment; (7) Review: To review systemically progress and unresolved problems in the field, comment on the state of current research, and make suggestions for future work; (8) Original Articles: To report innovative and original findings in radiology; (9) Brief Articles: To briefly report the novel and innovative findings in radiology; (10) Case Report: To report a rare or typical case; (11) Letters to the Editor: To discuss and make reply to the contributions published in *WJR*, or to introduce and comment on a controversial issue of general interest; (12) Book Reviews: To introduce and comment on quality monographs of radiology; and (13) Guidelines: To introduce consensuses and guidelines reached by international and national academic authorities worldwide on the research in radiology.

Name of journal

World Journal of Radiology

ISSN

ISSN 1949-8470 (online)

Indexed and Abstracted in

PubMed Central, PubMed, Digital Object Identifer, and Directory of Open Access Journals.

Published by

Baishideng Publishing Group Co., Limited.

SPECIAL STATEMENT

All articles published in this journal represent the viewpoints of the authors except where indicated otherwise.

Biostatistical editing

Statisital review is performed after peer review. We invite an expert in Biomedical Statistics from to evaluate the statistical method used in the paper, including *t*-test (group or paired comparisons), chi-squared test, Ridit, probit, logit, regression (linear, curvilinear, or stepwise), correlation, analysis of variance, analysis of covariance, *etc.* The reviewing points include: (1) Statistical methods should be described when they are used to verify the results; (2) Whether the statistical techniques are suitable or correct; (3) Only homogeneous data can be averaged. Standard deviations are preferred to standard errors. Give the number of observations and subjects (*n*). Losses in observations, such as drop-outs from the study should be reported; (4) Values such as ED50, LD50, IC50 should have their 95% confidence limits calculated and compared by weighted probit analysis (Bliss and Finney); and (5) The word 'significantly' should be replaced by its synonyms (if it indicates extent) or the *P* value (if it indicates statistical significance).

Conflict-of-interest statement

In the interests of transparency and to help reviewers assess any potential bias, *WJR* requires authors of all papers to declare any competing commercial, personal, political, intellectual, or religious interests in relation to the submitted work. Referees are also asked to indicate any potential conflict they might have reviewing a particular paper. Before submitting, authors are suggested to read "Uniform Requirements for Manuscripts Submitted to Biomedical Journals: Ethical Considerations in the Conduct and Reporting of Research: Conflicts of Interest" from International Committee of Medical Journal Editors (ICMJE), which is available at: http://www.icmje.org/ethical_4conflicts.html.

Sample wording: [Name of individual] has received fees for serving as a speaker, a consultant and an advisory board member for [names of organizations], and has received research funding from [names of organization]. [Name of individual] is an employee of [name of organization]. [Name of individual] owns stocks and shares in [name of organization]. [Name of individual] owns patent [patent identification and brief description].

Statement of informed consent

Manuscripts should contain a statement to the effect that all human studies have been reviewed by the appropriate ethics committee or it should be stated clearly in the text that all persons gave their informed consent prior to their inclusion in the study. Details that might disclose the identity of the subjects under study should be omitted. Authors should also draw attention to the Code of Ethics of the World Medical Association (Declaration of Helsinki, 1964, as revised in 2004).

Statement of human and animal rights

When reporting the results from experiments, authors should follow the highest standards and the trial should conform to Good Clinical Practice (for example, US Food and Drug Administration Good Clinical Practice in FDA-Regulated Clinical Trials; UK Medicines Research Council Guidelines for Good Clinical Practice in Clinical Trials) and/or the World Medical Association Declaration of Helsinki. Generally, we suggest authors follow the lead investigator's national standard. If doubt exists whether the research was conducted in accordance with the above standards, the authors must explain the rationale for their approach and demonstrate that the institutional review body explicitly approved the doubtful aspects of the study.

Before submitting, authors should make their study approved by the relevant research ethics committee or institutional review board. If human participants were involved, manuscripts must be accompanied by a statement that the experiments were undertaken with the understanding and appropriate informed consent of each. Any personal item or information will not be published without explicit consents from the involved patients. If experimental animals were used, the materials and methods (experimental procedures) section must clearly indicate that appropriate measures were taken to minimize pain or discomfort, and details of animal care should be provided.

SUBMISSION OF MANUSCRIPTS

Manuscripts should be typed in 1.5 line spacing and 12 pt. Book Antiqua with ample margins. Number all pages consecutively, and start each of the following sections on a new page: Title Page, Abstract, Introduction, Materials and Methods, Results, Discussion, Acknowledgements, References, Tables, Figures, and Figure Legends. Neither the editors nor the publisher are responsible for the opinions expressed by contributors. Manuscripts formally accepted for publication become the permanent property of Baishideng Publishing Group Co., Limited, and may not be reproduced by any means, in whole or in part, without the written permission of both the authors and the publisher. We reserve the right to copy-edit and put onto our website accepted manuscripts. Authors should follow the relevant guidelines for the care and use of laboratory animals of their institution or national animal welfare committee. For the sake of transparency in regard to the performance and reporting of clinical trials, we endorse the policy of the ICMJE to refuse to publish papers on clinical trial results if the trial was not recorded in a publicly-accessible registry at its outset. The only register now available, to our knowledge, is http://www.clinicaltrials.gov sponsored by the United States National Library of Medicine and we encourage all potential contributors to register with it. However, in the case that other registers become available you will be duly notified. A letter of recommendation from each author's organization should be provided with the contributed article to ensure the privacy and secrecy of research is protected.

Authors should retain one copy of the text, tables, photographs and illustrations because rejected manuscripts will not be returned to the author(s) and the editors will not be responsible for loss or damage to photographs and illustrations sustained during mailing.

Online submissions

Manuscripts should be submitted through the Online Submission System at: http://www.wjgnet.com/1949-8470office. Authors are highly recommended to consult the ONLINE INSTRUCTIONS TO AUTHORS (http://www.wjgnet.com/1949-8470/g_info_20100316162358.htm) before attempting to submit online. For assistance, authors encountering problems with the Online Submission System may send an email describing the problem to wjr@wjgnet.com, or by telephone: +86-10-85381892. If you submit your manuscript online, do not make a postal contribution. Repeated online submission for the same manuscript is strictly prohibited.

MANUSCRIPT PREPARATION

All contributions should be written in English. All articles must be submitted using word-processing software. All submissions must be typed in 1.5 line spacing and 12 pt. Book Antiqua with ample margins. Style should conform to our house format. Required information for each of the manuscript sections is as follows:

Title page

Title: Title should be less than 12 words.

Running title: A short running title of less than 6 words should be provided.

Authorship: Authorship credit should be in accordance with the standard proposed by International Committee of Medical Journal Editors, based on (1) substantial contributions to conception and design, acquisition of data, or analysis and interpretation of data; (2) drafting the article or revising it critically for important intellectual content; and (3) final approval of the version to be published. Authors should meet conditions 1, 2, and 3.

Institution: Author names should be given first, then the complete name of institution, city, province and postcode. For example, Xu-Chen Zhang, Li-Xin Mei, Department of Pathology, Chengde Medical College, Chengde 067000, Hebei Province, China. One author may be represented from two institutions, for example, George Sgourakis, Department of General, Visceral, and Transplantation Surgery, Essen 45122, Germany; George Sgourakis, 2nd Surgical

Department, Korgialenio-Benakio Red Cross Hospital, Athens 15451, Greece

Author contributions: The format of this section should be: Author contributions: Wang CL and Liang L contributed equally to this work; Wang CL, Liang L, Fu JF, Zou CC, Hong F and Wu XM designed the research; Wang CL, Zou CC, Hong F and Wu XM performed the research; Xue JZ and Lu JR contributed new reagents/analytic tools; Wang CL, Liang L and Fu JF analyzed the data; and Wang CL, Liang L and Fu JF wrote the paper.

Supportive foundations: The complete name and number of supportive foundations should be provided, e.g., Supported by National Natural Science Foundation of China, No. 30224801

Correspondence to: Only one corresponding address should be provided. Author names should be given first, then author title, affiliation, the complete name of institution, city, postcode, province, country, and email. All the letters in the email should be in lower case. A space interval should be inserted between country name and email address. For example, Montgomery Bissell, MD, Professor of Medicine, Chief, Liver Center, Gastroenterology Division, University of California, Box 0538, San Francisco, CA 94143, United States. montgomery.bissell@ucsf.edu

Telephone and fax: Telephone and fax should consist of +, country number, district number and telephone or fax number, e.g., Telephone: +86-10-85381892 Fax: +86-10-85381893

Peer reviewers: All articles received are subject to peer review. Normally, three experts are invited for each article. Decision for acceptance is made only when at least two experts recommend an article for publication. Reviewers for accepted manuscripts are acknowledged in each manuscript, and reviewers of articles which were not accepted will be acknowledged at the end of each issue. To ensure the quality of the articles published in *WJR*, reviewers of accepted manuscripts will be announced by publishing the name, title/position and institution of the reviewer in the footnote accompanying the printed article. For example, reviewers: Professor Jing-Yuan Fang, Shanghai Institute of Digestive Disease, Shanghai, Affiliated Renji Hospital, Medical Faculty, Shanghai Jiaotong University, Shanghai, China; Professor Xin-Wei Han, Department of Radiology, The First Affiliated Hospital, Zhengzhou University, Zhengzhou, Henan Province, China; and Professor Anren Kuang, Department of Nuclear Medicine, Huaxi Hospital, Sichuan University, Chengdu, Sichuan Province, China.

Abstract

There are unstructured abstracts (no more than 256 words) and structured abstracts (no more than 480). The specific requirements for structured abstracts are as follows:

An informative, structured abstracts of no more than 480 words should accompany each manuscript. Abstracts for original contributions should be structured into the following sections. AIM (no more than 20 words): Only the purpose should be included. Please write the aim as the form of "To investigate/study/…; MATERIALS AND METHODS (no more than 140 words); RESULTS (no more than 294 words): You should present *P* values where appropriate and must provide relevant data to illustrate how they were obtained, e.g. 6.92 ± 3.86 *vs* 3.61 ± 1.67, $P < 0.001$; CONCLUSION (no more than 26 words).

Key words

Please list 5-10 key words, selected mainly from *Index Medicus*, which reflect the content of the study.

Text

For articles of these sections, original articles and brief articles, the main text should be structured into the following sections: INTRODUCTION, MATERIALS AND METHODS, RESULTS and DISCUSSION, and should include appropriate Figures and Tables. Data should be presented in the main text or in Figures and Tables, but not in both. The main text format of these sections, editorial, topic highlight, case report, letters to the editors, can be found at: http://www.wjgnet.com/1949-8470/g_info_20100313183720.htm.

Illustrations

Figures should be numbered as 1, 2, 3, *etc.*, and mentioned clearly in the main text. Provide a brief title for each figure on a separate page. Detailed legends should not be provided under the figures. This part should be added into the text where the figures are applicable. Figures should be either Photoshop or Illustrator files (in tiff, eps, jpeg formats) at high-resolution. Examples can be found at: http://www.wjgnet.com/1007-9327/13/4520.pdf; http://www.wjgnet.com/1007-9327/13/4554.pdf; http://www.wjgnet.com/1007-9327/13/4891.pdf; http://www.wjgnet.com/1007-9327/13/4986.pdf; http://www.wjgnet.com/1007-9327/13/4498.pdf. Keeping all elements compiled is necessary in line-art image. Scale bars should be used rather than magnification factors, with the length of the bar defined in the legend rather than on the bar itself. File names should identify the figure and panel. Avoid layering type directly over shaded or textured areas. Please use uniform legends for the same subjects. For example: Figure 1 Pathological changes in atrophic gastritis after treatment. A: ...; B: ...; C: ...; D: ...; E: ...; F: ...; G: …*etc.* It is our principle to publish high resolution-figures for the printed and E-versions.

Tables

Three-line tables should be numbered 1, 2, 3, *etc.*, and mentioned clearly in the main text. Provide a brief title for each table. Detailed legends should not be included under tables, but rather added into the text where applicable. The information should complement, but not duplicate the text. Use one horizontal line under the title, a second under column heads, and a third below the Table, above any footnotes. Vertical and italic lines should be omitted.

Notes in tables and illustrations

Data that are not statistically significant should not be noted. $^{a}P < 0.05$, $^{b}P < 0.01$ should be noted ($P > 0.05$ should not be noted). If there are other series of *P* values, $^{c}P < 0.05$ and $^{d}P < 0.01$ are used. A third series of *P* values can be expressed as $^{e}P < 0.05$ and $^{f}P < 0.01$. Other notes in tables or under illustrations should be expressed as ^{1}F, ^{2}F, ^{3}F; or sometimes as other symbols with a superscript (Arabic numerals) in the upper left corner. In a multi-curve illustration, each curve should be labeled with ●, ○, ■, □, ▲, △, *etc.*, in a certain sequence.

Acknowledgments

Brief acknowledgments of persons who have made genuine contributions to the manuscript and who endorse the data and conclusions should be included. Authors are responsible for obtaining written permission to use any copyrighted text and/or illustrations.

REFERENCES

Coding system

The author should number the references in Arabic numerals according to the citation order in the text. Put reference numbers in square brackets in superscript at the end of citation content or after the cited author's name. For citation content which is part of the narration, the coding number and square brackets should be typeset normally. For example, "Crohn's disease (CD) is associated with increased intestinal permeability[1,2]". If references are cited directly in the text, they should be put together within the text, for example, "From references[19,22-24], we know that..."

When the authors write the references, please ensure that the order in text is the same as in the references section, and also ensure the spelling accuracy of the first author's name. Do not list the same citation twice.

PMID and DOI

Pleased provide PubMed citation numbers to the reference list, e.g. PMID and DOI, which can be found at http://www.ncbi.nlm.nih.gov/sites/entrez?db=pubmed and http://www.crossref.org/SimpleTextQuery/, respectively. The numbers will be used in E-version of this journal.

Style for journal references

Authors: the name of the first author should be typed in bold-faced letters. The family name of all authors should be typed with the initial letter capitalized, followed by their abbreviated first and middle initials. (For example, Lian-Sheng Ma is abbreviated as Ma LS, Bo-Rong Pan as Pan BR). The title of the cited article and italicized journal title (journal title should be in its abbreviated form as shown in PubMed), publication date, volume number (in black), start page, and end page [PMID: 11819634 DOI: 10.3748/wjg.13.5396].

Style for book references

Authors: the name of the first author should be typed in bold-faced letters. The surname of all authors should be typed with the initial letter capitalized, followed by their abbreviated middle and first initials. (For example, Lian-Sheng Ma is abbreviated as Ma LS, Bo-Rong Pan as Pan BR) Book title. Publication number. Publication place: Publication press, Year: start page and end page.

Format

Journals

English journal article (list all authors and include the PMID where applicable)

1 **Jung EM**, Clevert DA, Schreyer AG, Schmitt S, Rennert J, Kubale R, Feuerbach S, Jung F. Evaluation of quantitative contrast harmonic imaging to assess malignancy of liver tumors: A prospective controlled two-center study. *World J Gastroenterol* 2007; **13**: 6356-6364 [PMID: 18081224 DOI: 10.3748/wjg.13.6356]

Chinese journal article (list all authors and include the PMID where applicable)

2 **Lin GZ**, Wang XZ, Wang P, Lin J, Yang FD. Immunologic effect of Jianpi Yishen decoction in treatment of Pixu-diarrhoea. *Shijie Huaren Xiaohua Zazhi* 1999; **7**: 285-287

In press

3 **Tian D**, Araki H, Stahl E, Bergelson J, Kreitman M. Signature of balancing selection in Arabidopsis. *Proc Natl Acad Sci USA* 2006; In press

Organization as author

4 **Diabetes Prevention Program Research Group**. Hypertension, insulin, and proinsulin in participants with impaired glucose tolerance. *Hypertension* 2002; **40**: 679-686 [PMID: 12411462 PMCID:2516377 DOI:10.1161/01.HYP.0000035706.28494.09]

Both personal authors and an organization as author

5 **Vallancien G**, Emberton M, Harving N, van Moorselaar RJ; Alf-One Study Group. Sexual dysfunction in 1, 274 European men suffering from lower urinary tract symptoms. *J Urol* 2003; **169**: 2257-2261 [PMID: 12771764 DOI:10.1097/01.ju.0000067940.76090.73]

No author given

6 21st century heart solution may have a sting in the tail. *BMJ* 2002; **325**: 184 [PMID: 12142303 DOI:10.1136/bmj.325.7357.184]

Volume with supplement

7 **Geraud G**, Spierings EL, Keywood C. Tolerability and safety of frovatriptan with short- and long-term use for treatment of migraine and in comparison with sumatriptan. *Headache* 2002; **42** Suppl 2: S93-99 [PMID: 12028325 DOI:10.1046/j.1526-4610.42.s2.7.x]

Issue with no volume

8 **Banit DM**, Kaufer H, Hartford JM. Intraoperative frozen section analysis in revision total joint arthroplasty. *Clin Orthop Relat Res* 2002; (**401**): 230-238 [PMID: 12151900 DOI:10.1097/00003086-200208000-00026]

No volume or issue

9 Outreach: Bringing HIV-positive individuals into care. *HRSA Careaction* 2002; 1-6 [PMID: 12154804]

Books

Personal author(s)

10 **Sherlock S**, Dooley J. Diseases of the liver and billiary system. 9th ed. Oxford: Blackwell Sci Pub, 1993: 258-296

Chapter in a book (list all authors)

11 **Lam SK**. Academic investigator's perspectives of medical treatment for peptic ulcer. In: Swabb EA, Azabo S. Ulcer disease: investigation and basis for therapy. New York: Marcel Dekker, 1991: 431-450

Author(s) and editor(s)

12 **Breedlove GK**, Schorfheide AM. Adolescent pregnancy. 2nd ed. Wieczorek RR, editor. White Plains (NY): March of Dimes Education Services, 2001: 20-34

Conference proceedings

13 **Harnden P**, Joffe JK, Jones WG, editors. Germ cell tumours V. Proceedings of the 5th Germ cell tumours Conference; 2001 Sep 13-15; Leeds, UK. New York: Springer, 2002: 30-56

Conference paper

14 **Christensen S**, Oppacher F. An analysis of Koza's computational effort statistic for genetic programming. In: Foster JA, Lutton E, Miller J, Ryan C, Tettamanzi AG, editors. Genetic programming. EuroGP 2002: Proceedings of the 5th European Conference on Genetic Programming; 2002 Apr 3-5; Kinsdale, Ireland. Berlin: Springer, 2002: 182-191

Electronic journal (list all authors)

15 Morse SS. Factors in the emergence of infectious diseases. Emerg Infect Dis serial online, 1995-01-03, cited 1996-06-05; 1(1): 24 screens. Available from: URL: http://www.cdc.gov/ncidod/eid/index.htm

Patent (list all authors)

16 **Pagedas AC**, inventor; Ancel Surgical R&D Inc., assignee. Flexible endoscopic grasping and cutting device and positioning tool assembly. United States patent US 20020103498. 2002 Aug 1

Statistical data

Write as mean ± SD or mean ± SE.

Statistical expression

Express *t* test as *t* (in italics), *F* test as *F* (in italics), chi square test as χ^2 (in Greek), related coefficient as *r* (in italics), degree of freedom as υ (in Greek), sample number as *n* (in italics), and probability as *P* (in italics).

Units

Use SI units. For example: body mass, m (B) = 78 kg; blood pressure, p (B) = 16.2/12.3 kPa; incubation time, t (incubation) = 96 h, blood glucose concentration, c (glucose) 6.4 ± 2.1 mmol/L; blood CEA mass concentration, p (CEA) = 8.6 24.5 μg/L; CO_2 volume fraction, 50 mL/L CO_2, not 5% CO_2; likewise for 40 g/L formaldehyde, not 10% formalin; and mass fraction, 8 ng/g, *etc.* Arabic numerals such as 23, 243, 641 should be read 23 243 641.

The format for how to accurately write common units and quantums can be found at: http://www.wjgnet.com/1949-8470/g_info_20100313185816.htm.

Abbreviations

Standard abbreviations should be defined in the abstract and on first mention in the text. In general, terms should not be abbreviated unless they are used repeatedly and the abbreviation is helpful to the reader. Permissible abbreviations are listed in Units, Symbols and Abbreviations: A Guide for Biological and Medical Editors and Authors (Ed. Baron DN, 1988) published by The Royal Society of Medicine, London. Certain commonly used abbreviations, such as DNA, RNA, HIV, LD50, PCR, HBV, ECG, WBC, RBC, CT, ESR, CSF, IgG, ELISA, PBS, ATP, EDTA, mAb, can be used directly without further explanation.

Italics
Quantities: *t* time or temperature, *c* concentration, *A* area, *l* length, *m* mass, *V* volume.
Genotypes: *gyrA*, *arg* 1, *c myc*, *c fos*, *etc.*
Restriction enzymes: *Eco*RI, *Hin*dI, *Bam*HI, *Kbo* I, *Kpn* I, *etc.*
Biology: *H. pylori*, *E coli*, *etc.*

Examples for paper writing
Editorial: http://www.wjgnet.com/1949-8470/g_info_20100313182341.htm

Frontier: http://www.wjgnet.com/1949-8470/g_info_2010031318 2448.htm

Topic highlight: http://www.wjgnet.com/1949-8470/g_info_201003 13182639.htm

Observation: http://www.wjgnet.com/1949-8470/g_info_20100313 182834.htm

Guidelines for basic research: http://www.wjgnet.com/1949-8470/g_info_20100313183057.htm

Guidelines for clinical practice: http://www.wjgnet.com/1949-8470/g_info_20100313183238.htm

Review: http://www.wjgnet.com/1949-8470/g_info_20100313 183433.htm

Original articles: http://www.wjgnet.com/1949-8470/g_info_2010 0313183720.htm

Brief articles: http://www.wjgnet.com/1949-8470/g_info_201003 13184005.htm

Case report: http://www.wjgnet.com/1949-8470/g_info_20100313 184149.htm

Letters to the editor: http://www.wjgnet.com/1949-8470/g_info_20 100313184410.htm

Book reviews: http://www.wjgnet.com/1949-8470/g_info_201003 13184803.htm

Guidelines: http://www.wjgnet.com/1949-8470/g_info_20100313 185047.htm

SUBMISSION OF THE REVISED MANUSCRIPTS AFTER ACCEPTED

Please revise your article according to the revision policies of *WJR*. The revised version including manuscript and high-resolution image figures (if any) should be re-submitted or uploaded online. The author should send copyright transfer letter, and responses to the reviewers and science news to us *via* email.

Editorial Office

World Journal of Radiology
Editorial Department: Room 903, Building D,
Ocean International Center, No. 62 Dongsihuan Zhonglu,
Chaoyang District, Beijing 100025, China
E-mail: wjr@wjgnet.com
http://www.wjgnet.com
Telephone: +86-10-8538-1892
Fax: +86-10-8538-1893

Language evaluation
The language of a manuscript will be graded before it is sent for revision. (1) Grade A: priority publishing; (2) Grade B: minor language polishing; (3) Grade C: a great deal of language polishing needed; and (4) Grade D: rejected. Revised articles should reach Grade A or B.

Copyright assignment form
Please download a Copyright assignment form from http://www.wjgnet.com/1949-8470/g_info_20100313185522.htm.

Responses to reviewers
Please revise your article according to the comments/suggestions provided by the reviewers. The format for responses to the reviewers' comments can be found at: http://www.wjgnet.com/1949-8470/g_info_20100313185358.htm.

Proof of financial support
For paper supported by a foundation, authors should provide a copy of the document and serial number of the foundation.

Links to documents related to the manuscript
WJR will be initiating a platform to promote dynamic interactions between the editors, peer reviewers, readers and authors. After a manuscript is published online, links to the PDF version of the submitted manuscript, the peer-reviewers' report and the revised manuscript will be put on-line. Readers can make comments on the peer reviewer's report, authors' responses to peer reviewers, and the revised manuscript. We hope that authors will benefit from this feedback and be able to revise the manuscript accordingly in a timely manner.

Science news releases
Authors of accepted manuscripts are suggested to write a science news item to promote their articles. The news will be released rapidly at EurekAlert/AAAS (http://www.eurekalert.org). The title for news items should be less than 90 characters; the summary should be less than 75 words; and main body less than 500 words. Science news items should be lawful, ethical, and strictly based on your original content with an attractive title and interesting pictures.

Publication fee
WJR is an international, peer-reviewed, Open-Access, online journal. Articles published by this journal are distributed under the terms of the Creative Commons Attribution Non-commercial License, which permits use, distribution, and reproduction in any medium, provided the original work is properly cited, the use is non commercial and is otherwise in compliance with the license. Authors of accepted articles must pay a publication fee. The related standards are as follows. Publication fee: 1300 USD per article; Reprints fee: 350 USD per 100 reprints, including postage cost. Editorial, topic highlights, book reviews and letters to the editor are published free of charge.